9

STRUCTURE AND REACTIVITY OF DIOL HOST-GUEST COMPOUNDS

A Thesis submitted to the
UNIVERSITY OF CAPE TOWN
in fulfilment of the requirements for the degree of
MASTER OF SCIENCE

by

GRANT ANDREW HARVEY
B.Sc. (Hons) (Cape Town)

Department of Chemistry
University of Cape Town
Rondebosch
7700
South Africa

April 1990

ACKNOWLEDGEMENTS

I would like to thank the following people for their help during my M.Sc. project:

Professor L.R. Nassimbeni for his assistance and supervision.

Professor M.R. Caira for his tireless help, good humour and the exemplary standards he set.

Dr D.R. Bond for many fruitful discussions, proof-reading and valued friendship.

Dr M. Niven for the data collections.

Long Room Colleagues for companionship and especially Leonard, for his help with computations.

My parents for supporting me all these years.

Alexandra Bannatyne for her love and encouragement.

PUBLICATIONS

The essence of this thesis has been submitted to *Acta Crystallogr. B* for publication. The title of the paper is:

Complexation with diol host compounds. Part 5.
Structures and thermal analysis of trans-9,10-dihydroxy-9,10-diphenyl-9,10-dihydroanthracene with 2-butanone, 4-vinylpyridine, 4-methylpyridine and 2-methylpyridine.
D.R. Bond, M.R. Caira, G.A. Harvey, L.R. Nassimbeni and F. Toda.

ABSTRACT

The crystal structures of trans-9,10-dihydroxy-9,10-diphenyl-9,10-dihydroanthracene with various guest molecules have been determined by X-ray diffraction. The guests were 2-butanone, 4-vinylpyridine, 4-methylpyridine and 2-methylpyridine. The host to guest ratios were determined by microanalysis and density measurements.

The change of the overall host lattice structure upon guest release was studied by X-ray powder diffraction. The thermal characteristics of the compounds were studied using thermogravimetric analysis and differential scanning calorimetry.

Guest desorption from three of the four compounds occurred in a single step whereupon the host framework collapsed back to the guest-free structure.

The compound containing 4-methylpyridine, released the guest molecules in a two-step process. Evidence of a new host phase was identified from the XRD pattern of this intermediate phase. On further guest release, the intermediate phase converted to the guest-free host structure.

In an attempt to reconcile thermodynamics with structure, the correlation between hydrogen bond length and guest desorption enthalpy was investigated.

ABBREVIATIONS USED IN THE TEXT

b.p.	Boiling point
DSC	Differential scanning calorimetry
G	Guest
G.C.	Gas chromatography
H	Host
Me	Methyl ($-CH_3$)
m.p.	Melting point
s.o.f.	Site occupancy factor
TGA	Thermogravimetric analysis
XRD	X-ray powder diffraction

CONTENTS

Page No.

Page No.

CHAPTER ONE

INTRODUCTION

1. INTRODUCTION

1.1. Clathrate History

Clathrates and inclusion compounds were first described by Powell [1] in 1948 in a paper on the structure of β-quinol with sulphur dioxide. In this report he used the word clathrate to describe the inclusion of small guest molecules into the vacant spaces of the host structural framework leaving the bonding systems of both components unaffected. The history of compounds, now known as inclusion compounds, dates back to 1811 [2]. In 1823 Faraday reported the preparation of the chlorine clathrate hydrate [3]. Other pre-1948 reports on inclusion compounds include the following preparations: 1841 - graphite intercalates [4], 1849 - β-quinol H_2S clathrate [5], 1891 - cyclodextrin inclusion compounds [6], 1897 - nickel cyanide ammonia with benzene (Hofmann's inclusion compound) [7], 1906 - inclusion compounds of triphenylmethane [8], 1909 - tri-o-thymotide benzene inclusion compound [9], 1914 - clathrates of Dianin's compound [10], 1916 - inclusion compounds of the choleic acids [11], 1935 - phenol clathrates [12], 1940 - urea inclusion compounds [13], 1946 - amylase inclusion compounds [14].

1.2. Classification

Since 1948 when X-ray crystallography was applied as a tool to understand inclusion compounds, the interest in and hence the number of reports on clathrates has grown tremendously. As a result of this, a large number of descriptions of inclusion compounds ~~have~~ has been used but not precisely defined. This resulted in Weber and Josel [15,16] proposing a systematic classification based on the host-guest type and interaction, the topology of the host-guest aggregate and lastly on the number of various components forming the aggregate.

There are two main divisions based on the host-guest interaction. Complexes have coordination between host and guest while clathrates are complexes where the guest is retained by steric barriers (crystal lattice forces). Examples of complexes are the encapsulation of ions by crown ethers (Figure 1.1) and cryptands (Figure 1.2) while Dianin's compound (Figure 1.3) and urea (Figure 1.4) are examples of clathrates. Another distinguishing factor is that complexes retain their identity in solution, whereas clathrates normally decompose on dissolution.

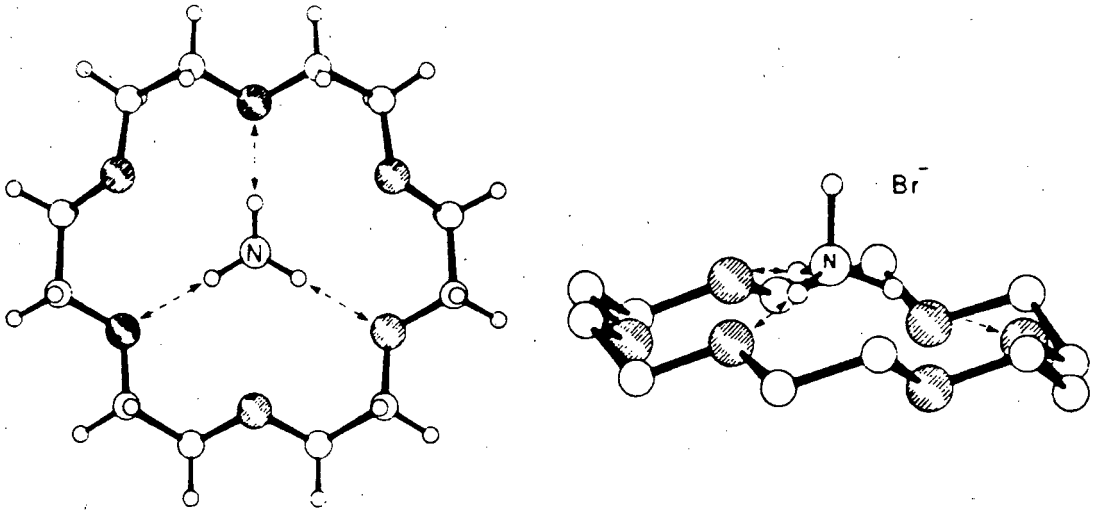

Figure 1.1 Two views of the host-guest association between 18-crown-6 and ammonium bromide. Hydrogen bonds are represented by arrows [17].

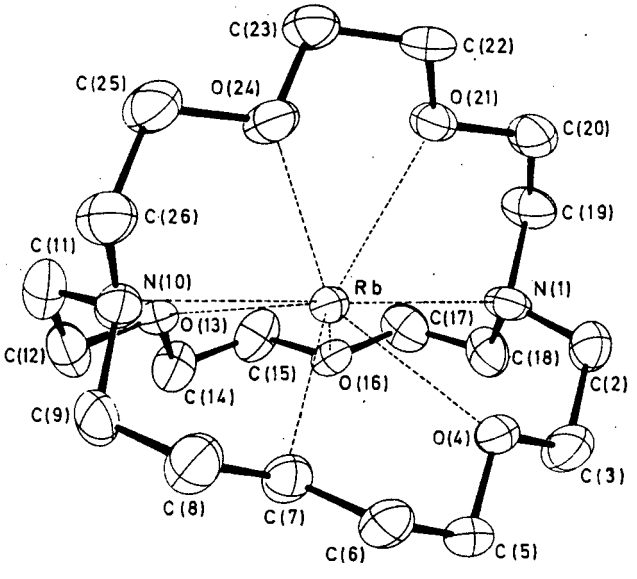

Figure 1.2 A rubidium 'cryptate', the complex cation $[RbC_{18}H_{36}N_2O_6]^+$ in the crystalline thiocyanate monohydrate [18].

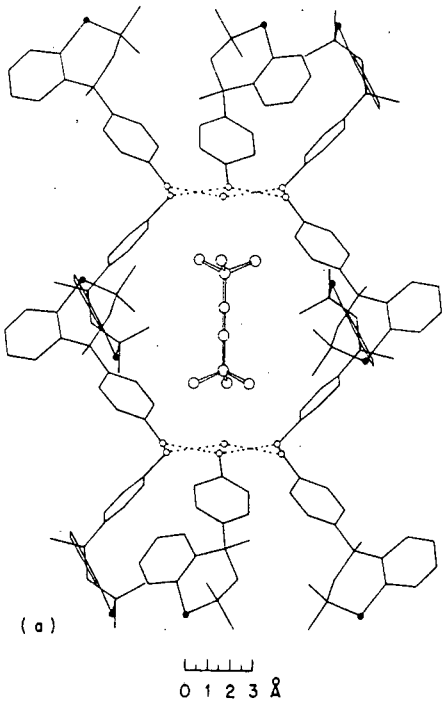

Figure 1.3 Dianin's compound: a view normal to the c-axis of 4-*p*-hydroxyphenyl-2,2,4-trimethylthiachroman. Two host molecules have been excluded (apart from their oxygen atoms) to reveal the guest 2,5,5-trimethylhex-3-yn-2-ol [19].

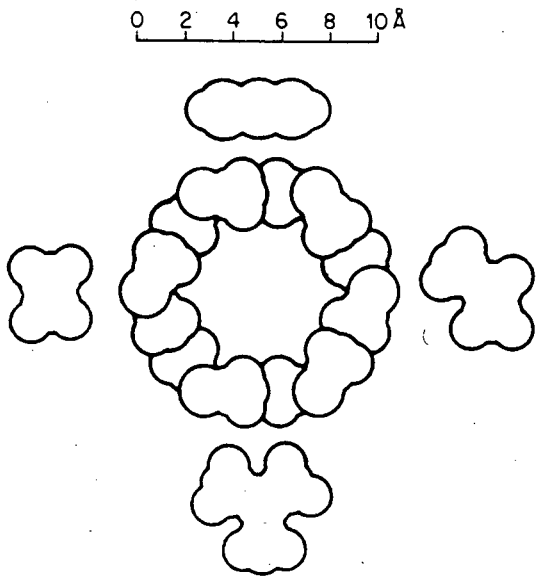

Figure 1.4 Cross section of the cavity in the urea channel compound with the size of n-octane (left), benzene (top), 3-methylheptane (right), and 2,2,4-trimethylpentane (bottom) [20].

Inclusion compounds do not always fall neatly into these two divisions and so two more classes have been introduced to deal with these complex/clathrate hybrids. *Coordinatoclathrates* display some degree of coordinative participation but have a dominant clathrate character and *Clathratocomplexes* are just the opposite.

The topology of the host-guest aggregate is divided as follows: intramolecular host-guest aggregates which contain any sort of host cavity are called *cavitates*, extramolecular host-guest aggregates containing a host cavity are termed *clathrates* and extramolecular host-guest aggregates which have no cavity or coordination are called *adducts*.

The topological characterisation can be defined further into five classes according to the shape and the dimensions of the host cavity. These classes, listed in decreasing order of encapsulation are: totally enclosed cage structures (*cryptates*), pocket or niche-like host arrangement (*aediculates*), one-dimensional open channel structures (*tubulates*), ring-like host cavities (*coordinates*) and the two-dimensional open layer or sandwich-type inclusion compounds (*intercalates*).

A further numerical classification according to the number of components in an aggregate can also be applied. The terms binary and ternary refer to a two or three component system respectively. The host:guest ratio can also be illustrated and a 1:2 host:guest ratio would be described as monomolecular binuclear.

It is also possible to distinguish between a guest-free host lattice and the appropriate host-guest compound by using the specific terminations *and* and *ate* respectively. Examples of this are cavit*ate*, tubul*ate* and clathr*ate* for host-guest compounds and cavit*and*, tubul*and* and clathr*and* for their respective guest-free host lattices.

1.3. Examples of well documented Inclusion Compounds

a) Graphite (Figure 1.5), one of the carbon allotropes, is the simplest compound to have a layered structure [22] and is classified as an intercalate. It has planar hexagonal carbon lattice layers stacked one on top of the other. The weak van der Waals interlayer forces allow guest atoms or molecules to reversibly penetrate between the layers by increasing the interplanar distance. Examples of

various guests are K, CrO_3, SbF_5 and $AlCl_3$ [22].

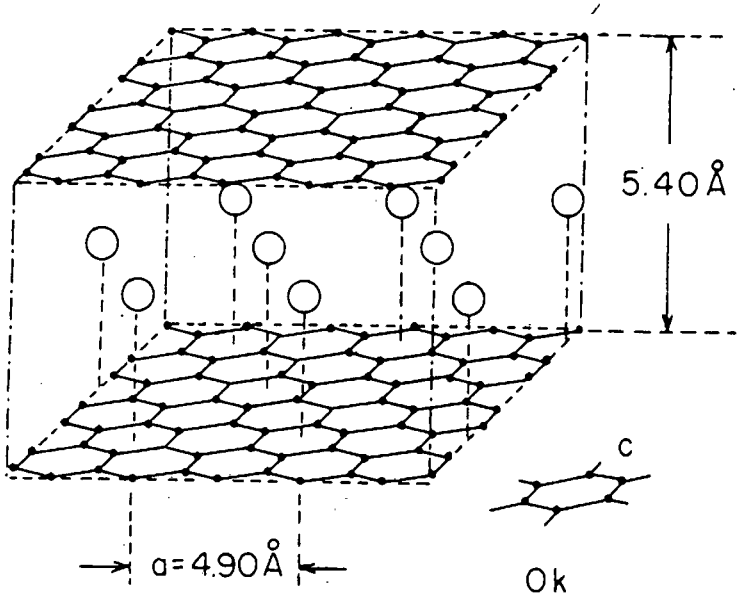

Figure 1.5 Potassium in graphite - C_8K. The interplanar distance of graphite has increased from 3.35Å to 5.40Å to accommodate the K atoms [21].

Intercalate type compounds display guest selectivity depending on the size of the guest molecule or the stereochemistry around the reaction centre imposed by the interlayer spacing limitation. Other examples of intercalates are layered silicates, used to achieve a variety of selective chemical conversions [23], and Li/TiS_2, showing possible use in battery systems [24].

b) Hofmann-type inclusion compounds (cryptates) can be viewed as being modified intercalates. Essentially they consist of planar layers containing metal atoms and cyanide groups with NH_3 groups protruding above and below the planes. These ammonia ligands act as blocking groups reducing the interplanar mobility of the guest and define a void wherein the guest molecule can be accommodated [22]. The basic Hofmann-type host lattice $Ni(NH_3)_2Ni(CN)_4$ can accommodate benzene (Figure 1.6) but not toluene as the interplanar distance is essentially fixed. By changing the ligands attached to the metal atom the guest selectivity could be altered.

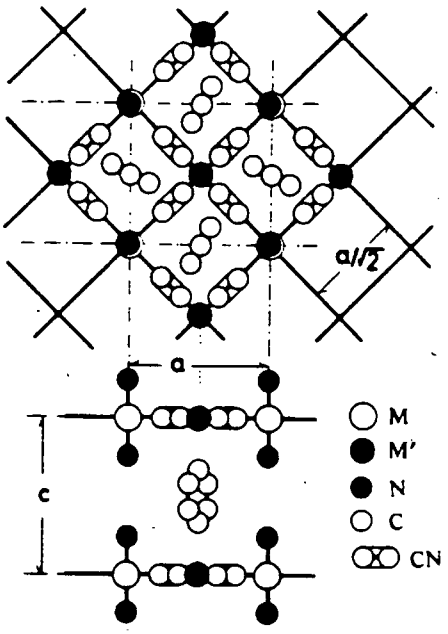

Figure 1.6 The structure of Hofmann-type clathrate $M(NH_3)_2M'(CN)_4 \cdot 2C_6H_6$. M=M'=Ni. Protons of the benzene and ammonia are not shown [25].

c) Werner-type inclusion compounds (cryptates) are very similar to the Hofmann compounds. An example of a typical Werner clathrate is $Ni(4\text{-}MePy)_4(NCS)_2$ where the layers contain the nickel atoms and the four 4-methylpyridine (4-picoline) groups with the isothiocyanate groups protruding above and below the plane defining the lattice void. These lattice voids show selectivity toward disubstituted benzenes [26] resulting in their use in chromatographic separation [27,28].

d) Urea molecules undergo hydrogen bonding forming long helical chains which make up central hexagonal channels (tubulates). These open channels can accommodate straight chain hydrocarbons of six or more carbon atoms. Thiourea forms channels very similar to those of urea but having a channel diameter 0.85Å greater than urea [20] resulting in the thiourea being able to include highly branched hydrocarbons and some five-, six- and eight-membered ring compounds in addition to the straight chain hydrocarbons [29].

The chiral nature of the channel allows for separation of enantiomers [30] and polymerisation of unsaturated molecules into stereo-regular polymers [22,31].

e) Cyclodextrins are torus shaped cyclic oligosaccharides made up of α-1,4-linked d-glucopyranose units. The most common cyclodextrins, α, β and γ consist of six, seven, and eight glucose units respectively and have a height of above 8Å. The internal channel diameter varies from about 5Å in α-cyclodextrin to 8Å in γ-cyclodextrin (Figure 1.7) [22]. Depending on the stacking of successive host molecules the guest can be accommodated in cage-type or channel-type cavities resulting in these compounds being able to form many inclusion complexes [32]. Cyclodextrin inclusion compounds are stable in solution as well as the solid state and hence their investigation as biomimetic systems [22].

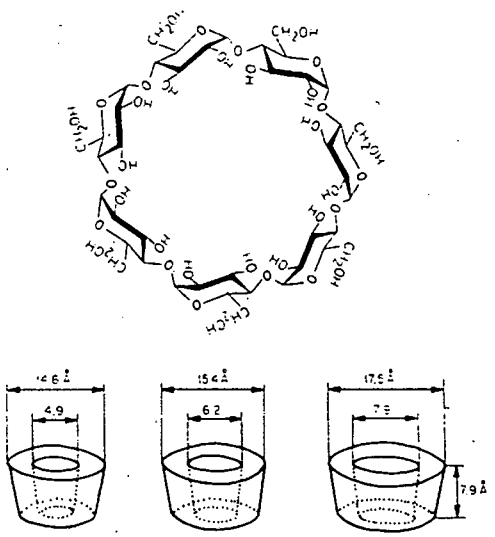

Figure 1.7 Structure of β-cyclodextrin, and molecular dimensions of α-, β-, γ-cyclodextrins [32].

A few of the uses of cyclodextrin inclusion compounds range from a cyclodextrin-peppermint complex used as a "longer lasting" flavourant in chewing gum [33], usefulness in rust prevention [34] to the use of the CO_2 clathrate of α-cyclodextrin as baking powder [35].

f) Dianin's compound consists of hexagonal units of OH groups hydrogen bonded in such a way that allows the oxygen atoms to form distorted hexagons with

alternate molecules of opposite configuration lying on opposite sides of its plane. Two such groups are stacked along the c axis such that their bulkier parts interlock forming a cage (Figure 1.3) [36]. The cage is hour-glass in shape and can retain many organic molecules as well as sulphur dioxide, iodine, ammonia and decalin [19]. The guest molecules in many Dianin's inclusion compounds are disordered and depending on their size, more than one guest molecule can be accommodated [36]. Dianin's inclusion compounds have been used in the separation of certain hydrocarbon mixtures [19]. The SF_6 clathrate is used as a convenient means of storage and controlled release of sulphur hexafluoride, a gas of considerable use in the electrical industry [19].

1.4. The importance of inclusion compounds and their resultant investigation

The important industrial objectives and applications of inclusion complexes are directed to chemical analysis and molecular separation. Depending on the size, shape and chemical nature of the holes generated in an inclusion lattice, certain guest molecules in a mixture, that best match the void conditions, would be selectively included. The separation of constitutional isomers, positional isomers, regioisomers, stereoisomers (both enantiomers and diastereomers) and even isotopic isomers could be envisaged [16].

The chemical reactivity (photo or thermal isomerisation) of a free substrate molecule may be dissimilar to one included in a lattice enclosure resulting from conformational differences [37,38]. In general, lattice inclusion will alter a guest molecule's physical properties [39]. This inclusion could ease the storage and handling problems of hazardous chemicals [40,41].
Up to the early 1980's the majority of host-guest compounds known had been chance discoveries. New host compounds were created by simple modification of known lattice formers. The host lattice cavity size can be varied by slight alterations of the host compound. An example of this is the modification of Dianin's compound by addition of a methyl group leading to a change in the cavity shape from "hour-glass" to "chinese lantern" (Figure 1.8). This cavity change results in a modified selectivity. Recently an increasing number of new compounds unrelated to previous host lattices have been designed based on the knowledge gained from known crystal structures.

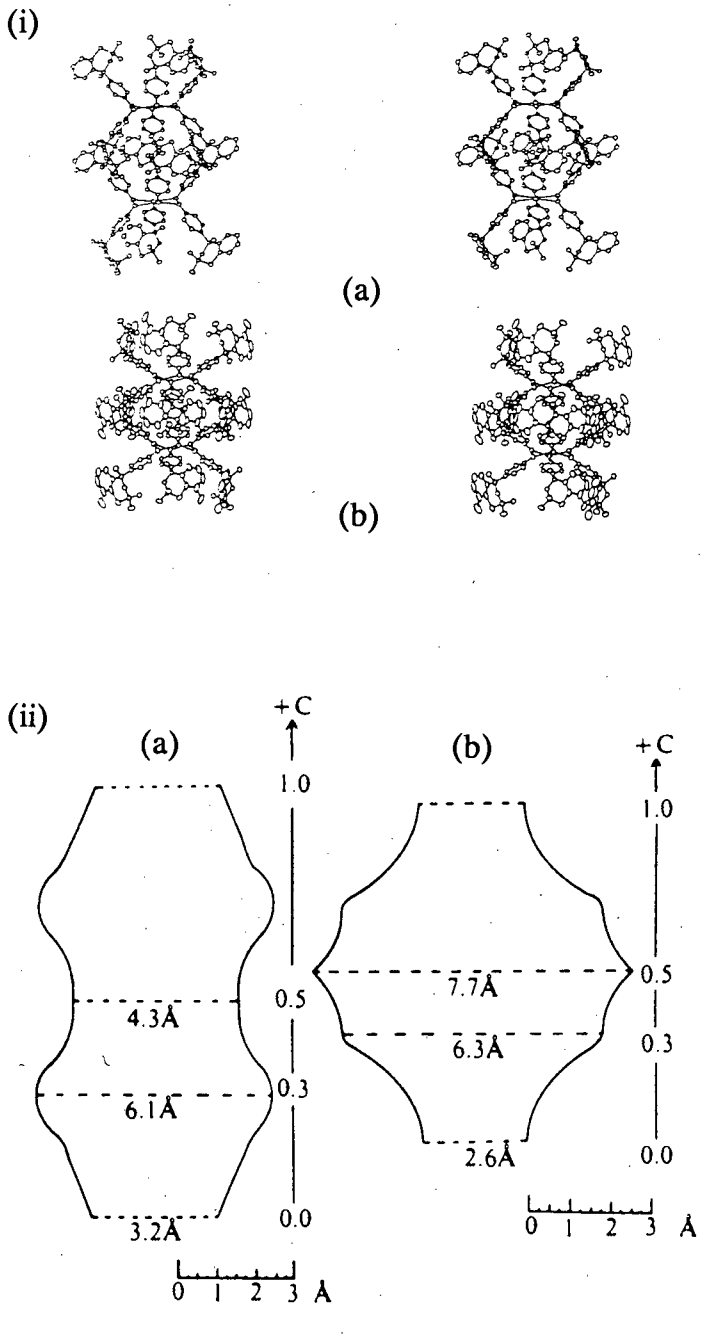

Figure 1.8 (i) Comparative stereoviews for (a) 4-*p*-hydrophenyl-2,2,4-trimethylthiachroman and (b) 4-*p*-hydrophenyl-2,2,4,8-tetramethylthiachroman and (ii) section through the van der Waals surface of (a) and (b) [19].

In the early seventies, MacNicol designed a new host family based on previously gathered knowledge [42]. He noticed that both quinol and Dianin's host lattices possess a hexagonal unit of hydrogen bonded hydroxyl groups and compared this with a hexasubstituted benzene (Figure 1.9). The z····z separation is very similar to the O····O distance of the hydroxy hexagon. By varying the substituent side arms, the inclusion cavity can be tuned to specific geometric and steric requirements.

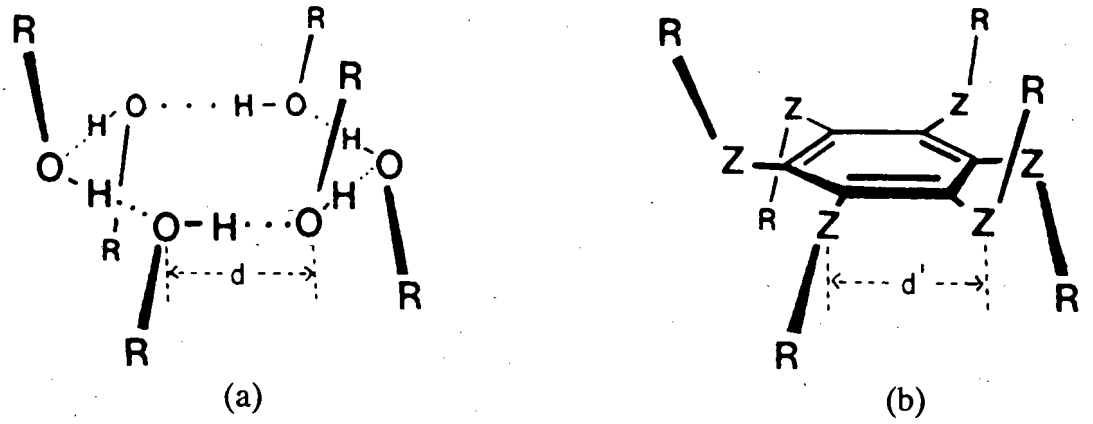

Figure 1.9 Comparison of (a) hydrogen-bonded hexamer unit with (b) hexasubstituted benzene analogue [43].

In 1968 Toda [44] started work on a new overall molecular shape with tetraphenyl-2,4-hexadiyne-1,6-diol. The design known as the "wheel and axle" contains a molecular axis of sp- carbons with sp^3- carbons at each end bearing relatively large spacer groups (phenyls). These spacer groups prevent close packing, leaving large lattice voids. The lattice dimensions can be altered by using a varying number of sp- carbons or substituting these with sp^2- or sp^3- carbons which would facilitate length variation and bending of the molecular axis. The terminal sp^3- carbons also bear hydroxyl groups which could contribute to inclusion formation by host-guest hydrogen bonding.

The knowledge gained from the study of X-ray crystallographic structures of various hydroxy host systems with a variety of alcohols and glycols [45-48] can be used for the rational design of new and more efficient host systems [45].

The X-ray crystallographic structures of the inclusion compounds of 1,1,6,6-tetraphenylhexa-2,4-diyne-1,6-diol (1a) and 1,1,4,4-tetraphenylbut-2-yne-1,4-diol (1b) (Figure 1.10) showed that they generally include guest species in the 1:2 and 1:1 host:guest ratio respectively [49]. This is attributed to (1a) having more space between the two diphenylcarbinol moieties and therefore having a larger lattice void in which to accommodate the guest. In all these inclusion compounds, strong hydrogen bonding presence is suggested by the lowering in absorption frequency of the OH bond from the uncomplexed to the complexed compounds.

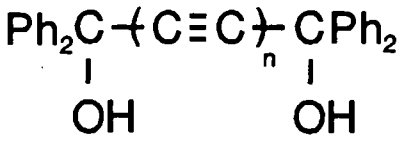

(1a): n=2

(1b): n=1

(1c): n=0

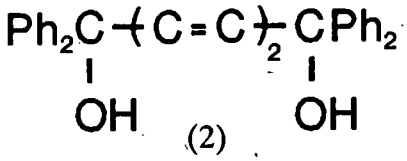

(2)

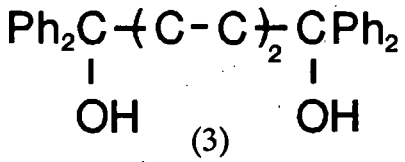

(3)

Figure 1.10

The compound 1,1,2,2-tetraphenyl-ethanediol (1c) (Figure 1.10) having even less space between diphenylcarbinol moieties than (1b) would not be expected to be a good host molecule. This does not prove to be the case as (1c) forms inclusion compounds with quite a few guests [49] but probably by a different mechanism from the (1a) and (1b) compounds. For example there is an absence of hydrogen bonding, with *p*-xylene surrounded by phenyl groups only, in the X-ray crystal structure of the 1:1 *p*-xylene inclusion compound with host (1c).

The rigidity of the molecular axis in these wheel-and-axle compounds is an important fact. There are only a few inclusion compounds of (E,E)-1,1,6,6-tetraphenylhexa-2,4-diene-1,6-diol (2) [49] and 1,1,6,6-tetraphenylhexane (3) does not form any inclusion compounds [49].

The rational design of a new host compound based on the above findings would include a rigid molecule with an anti-diol function and some bulky hydrophobic groups. *Trans*-9,10-dihydroxy-9,10-diphenyl-9,10-dihydroanthracene (H) (Figure 1.11) contains all these features as do other newly designed host compounds.

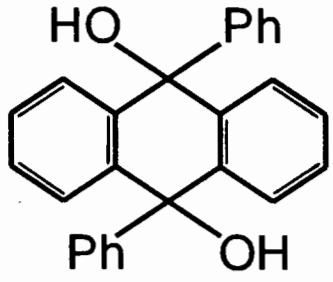

(H)

Figure 1.11 *Trans*-9,10-dihydroxy-9,10-diphenyl-9,10-dihydroanthracene, the host compound in all four compounds studied in this thesis.

This compound, (H), as well as many other hydroxy host compounds ~~have~~ has been found to form inclusion compounds with alcohols including ethanol [50]. If this inclusion phenomenon could be used as a cheap way to isolate ethanol from aqueous solution, obtained by the fermentation of biomass, this might provide a cheap source of energy. The extraction of ethanol from various concentrations of aqueous solution has been achieved using a number of hydroxy host compounds. These hydroxy compounds, of which *trans*-9,10-dihydroxy-9,10-diphenyl-9,10-dihydroanthracene is one, do not include water. The reason for water exclusion but alcohol inclusion as a guest, is the non-bonded interaction energy. The alcohol has a hydroxy group able to form a hydrogen bond as well as a hydrophobic alkyl group which can interact favourably with the hydrocarbon part of the host. Although water can also form hydrogen bonds with the host, it does not interact well with the host hydrophobic group [51]. A yield of 72% (based on the complex) was achieved from an 80% ethanol solution using 9-hydroxy-9-(1-propynyl)fluorene [50].

This separating ability could be extended to include separation of organic solvent mixtures. Upon dissolving the "unclathrated" α-phase *trans*-9,10-dihydroxy-9,10-

diphenyl-9,10-dihydroanthracene directly in the liquid guest, a new β- or "clathrate" phase is formed. Although the mechanism of this process is not fully understood, the guest molecule, because of its shape and resulting host-guest interaction, probably acts as a template for the new structure. Upon heating this β-phase host-guest complex, the guest molecules escape leading to three possibilities (Figure 1.12). The host may revert back to the α-phase, form a new γ-phase, or the host lattice could hold, giving rise to an *empty* "clathrate" referred to as the β_o-phase. This latter phenomenon is well known for zeolites, which can be dehydrated by heating to elevated temperatures under vacuum without significant damage to the silica/alumina framework [52].

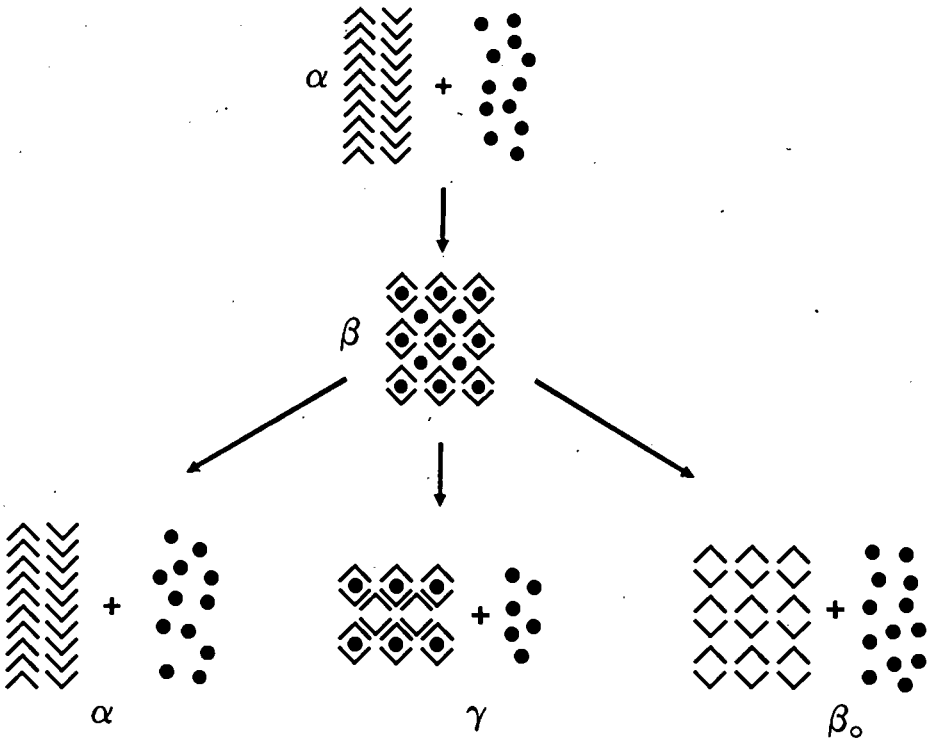

Figure 1.12 Schematic diagram showing possible decomposition paths of inclusion compounds.

If upon guest release from the β-phase host-guest complex, the host framework were to remain unbroken, this β_o-phase could then be extremely useful in the separation of the formerly included molecule type from a mixture of various organic solvents i.e. acting as a molecular "sieve" [53]. This separation could be

achieved by loading a wad of the host β_o-phase in a G.C. column and running the mixed organic solution through the chromatograph. The formerly included guest molecule type would be retarded in its movement along the column, relative to the other molecule types, as it would fit into the lattice voids of the host β_o-phase. This difference in retention time would enable separation of similar molecules having comparable boiling points.

The separation of 3-methylpyridine (b.p. 143.5°C) and 4-methylpyridine (b.p. 143.1°C) is industrially difficult. Compound (1c) only includes 3-picoline and so can be used to separate these picolines [49].

The X-ray crystallographic structures of *trans*-9,10-dihydroxy-9,10-diphenyl-9,10-dihydroanthracene [54] and its 1:2 methanol [54], 1:1 ethanol [48], 1:1 1,4-butanediol [45], 1:2 acetophenone [55], 1:2 3-methylcyclopentanone [55], 1:2 4-methylcyclohexanone [56], 1:2 2-methylcyclohexanone [56] inclusion complexes have been reported and the work discussed in this thesis adds to the accumulation of knowledge on these compounds.

CHAPTER TWO

AIM OF THIS PROJECT

CHAPTER THREE

EXPERIMENTAL

3. EXPERIMENTAL

3.1 Synthesis of Host $C_{26}H_{20}O_2$

The host complex previously synthesised by Ingold and Marshall [57] was prepared as follows:

A Grignard reagent was prepared by adding bromobenzene (10.4ml, 98.7mmol) in dry ether (30ml) dropwise, to magnesium (2.51g, 103mmol) in dry ether (10ml). The reaction mixture was refluxed for 90 minutes.

The Grignard reagent was then slowly added to a suspension of anthraquinone (4.05g, 19.5mmol) in dry ether (70ml) and refluxed for 20 hours. The reaction mixture was acidified on ice with 2M HCl to pH 2 and swirled for 20 minutes.

The resulting white precipitate (host powder complex) was filtered, twice recrystallised from benzene and dried in a desiccator for 24 hours. After the second recrystallisation, the mass of the pure white host (m.p. 261 - 263°C) was 2.63g (7.22mmol) representing a yield of 37% .
The microanalysis was as follows:

Calculated for $C_{26}H_{20}O_2$	C 85.9 %	H 5.2 %
Observed for $C_{26}H_{20}O_2$	C 85.7 %	H 5.5 %

3.2 Crystal growth

The host powder $C_{26}H_{20}O_2$, was dissolved in preheated guest solvent until saturation was achieved. The solution was diluted with guest solvent and allowed to cool to room temperature. In the case of the 2-butanone guest the solution was stoppered and left to stand whilst the other three solutions (4-vinylpyridine, 4-picoline and 2-picoline) were left open. The crystal growth time varied from two days, in the case of the 2-butanone, to a week for 2-picoline.

3.3. Preliminary Characterisation

3.3.1. Density measurements

Density measurements were made using the flotation method. Single crystals were suspended in a mixture of saturated aqueous KI and distilled water. When an approximate density measurement was obtained, a new crystal was suspended in the solution (as the original crystal became cloudy indicating guest loss) and the density of the solution measured using an Anton Paar digital density meter DMA 35. Density determination for each compound was performed in triplicate.

3.3.2. Microanalyses

C, H, and N analyses were performed on an Heraeus Universal combustion analyser Model CHN-RAPID [58].

These analyses had to be carried out quickly as these compounds decay by continuous guest desorption, when open to the atmosphere. The crystals were removed from their mother liquor and dabbed dry but not subjected to vacuum as this would have removed some of the guest, yielding inaccurate elemental analyses.

3.3.3. TGA , DSC and melting point determinations

The Thermogravimetric Analysis (TGA) measurements were performed using a Du Pont 9900 Thermogravimetric Analyser. The instrument was calibrated using $CuSO_4 \cdot 5H_2O$ as a standard. Water molecules were lost at 85°C ($2xH_2O$), 115°C ($2xH_2O$) and 230°C ($1xH_2O$) [59,60]. The samples, dabbed dry to remove surface solvent, ranging in mass between 6.07 and 13.97mg were placed in a platinum bucket and heated at a rate of 10°C/min from 20° to 350°C under a constant positive N_2 flow.

Differential Scanning Calorimetry (DSC) measurements were performed using a Du Pont 9900 Differential Scanning Calorimeter. The instrument was calibrated using Indium (ΔH = 28.4 J/g, m.p. = 156.7°C) [61] and Zinc (ΔH = 102.1 J/g, m.p. = 419.6°C) [62]. The samples ranging in mass between 6.2 and 12.6mg, dabbed dry to remove surface solvent, were placed on aluminium lids and heated

at a rate of 10°C/min from 20° to 350°C.

Melting point determinations were carried out using a Linkam TH600 hotstage with a Linkam CO600 temperature controller. A Nikon SMZ-10 microscope was used for viewing the melting process.

3.3.4. Guest desorption studies

The apparatus used for the desorption studies, represented diagrammatically in Figure 3.1, consisted essentially of a well calibrated McBain and Bakr [63] silica spring from which a thin foil bucket was suspended. The bucket was used as a container for the host-guest complex under investigation. The spring and bucket were enclosed in a water jacket which facilitated temperature control. The whole system was connected to a vacuum with the pressure measured using a M^{c}Leod gauge No 292.

The finely ground host-guest complex was placed in the bucket and the whole system sealed. This preparation was done as quickly as possible to minimize guest desorption into the atmosphere. The entire system was evacuated to ~2mmHg and the extension of the spring monitored. The bucket displacement is directly related to mass change by Hooke's Law:

$$F = -kx$$

F = restoring force = - mass x acceleration due to gravity
x = spring extension
k = spring constant
Thus, the guest loss from the host-guest complex could be monitored as a function of spring extension which is directly proportional to mass change.

Guest desorption was also achieved using a thermostat vacuum oven supplied by Townson and Mercer Ltd. The pre-weighed host-guest complex was placed in the oven, evacuated to 160mmHg and thermostated at various temperatures as discussed in Chapter 4. After a certain length of time the host-guest complex was reweighed and the mass loss calculated.

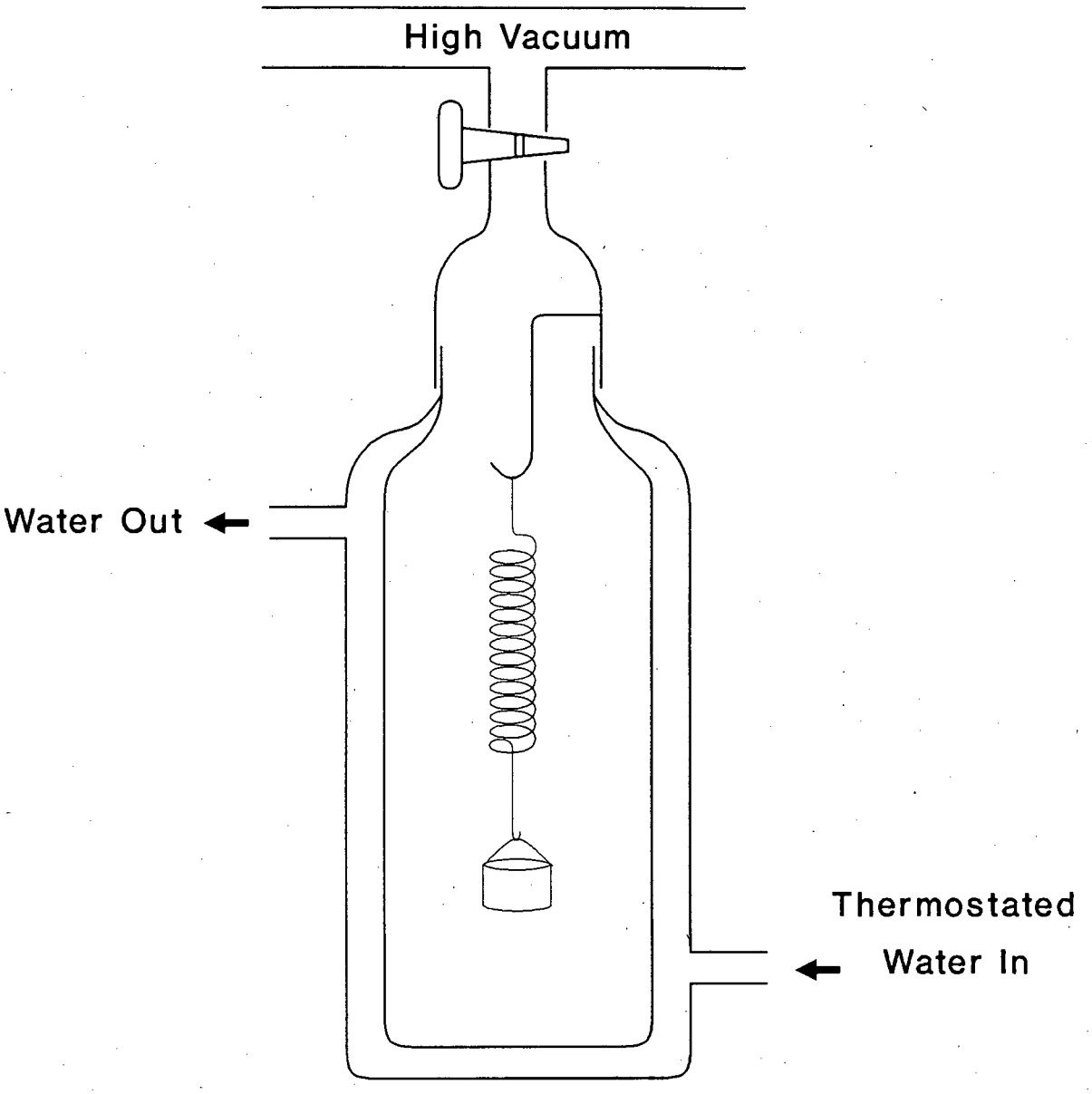

Figure 3.1 Schematic diagram of the apparatus used in the desorption studies.

3.3.5. X-ray powder diffraction

X-ray powder diffraction experiments were carried out using a Philips vertical goniometer PW1050/80 with a Philips PW1394 motor control and PW1390 channel control. The X-rays were generated by a Philips PW1130/90 model operating at 40kV and 30mA. Nickel-filtered copper radiation (CuKα, λ = 1.5418Å) was used with divergence and receiving slits of 1° each with no anti-scatter slit. The samples, dabbed dry to remove surface solvent, were ground into fine powder form, packed in a sample holder so as to minimise preferred orientation effects and scanned at 1°2θ/min over the range $8° \leq 2\theta \leq 40°$. The sensitivity range setting varied between 1×10^4 and 4×10^4 counts/s.

3.4. Single crystal X-ray diffraction

3.4.1. Crystal preparation

Single crystals of suitable size, selected on their ability to extinguish plane polarised light uniformly, were isolated or cut, and mounted in Lindemann capillary tubes to minimize deterioration by the desorption of the guest solvent.

In the case of compounds (I) and (IV) satisfactory photographs and data collections were obtained by mounting the crystals with mother liquor in 0.5mm diameter capillaries and sealing the tubes with wax. For compounds (II) and (III), the crystals were mounted in 0.3mm diameter capillaries and sealed by melting the ends with a naked flame.

Photographs of the crystals of compounds (III) and (IV) used for data collection are shown in Figure 3.2

3.4.2. Preliminary crystal X-ray photography

Preliminary cell parameters and space groups were established photographically using nickel-filtered CuKα radiation (λ = 1.5418Å) generated by Philips PW1120 and PW1140 X-ray generators operating at 20mA, 40kV and 40mA, 40kV respectively. The X-ray photographs were taken using a non-integrating Stoë goniometer for oscillation and Weissenberg photographs and a Stoë Reciprocal

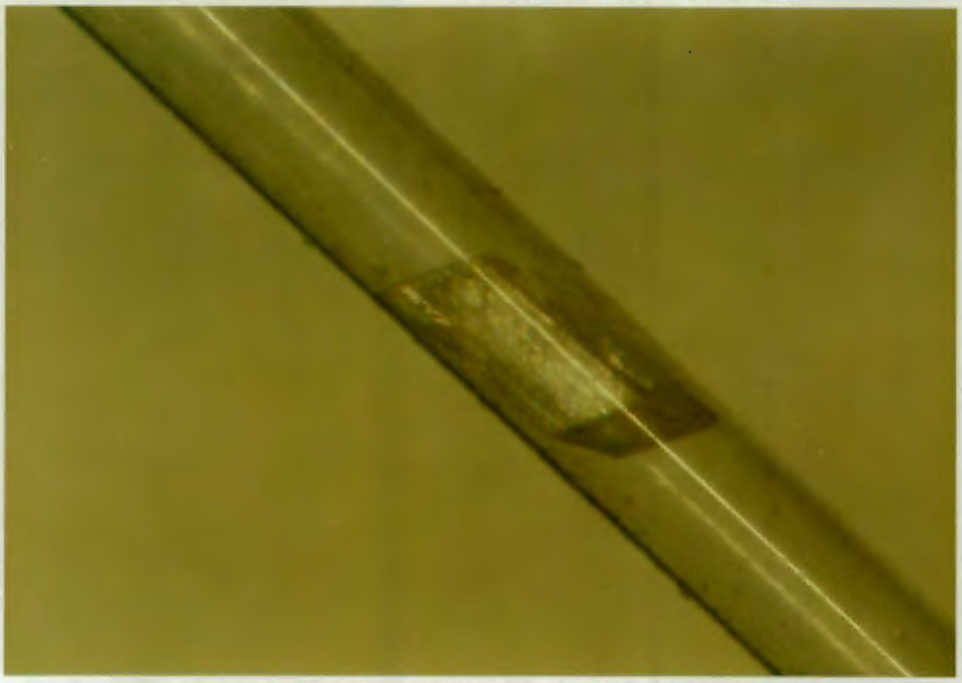

(a)

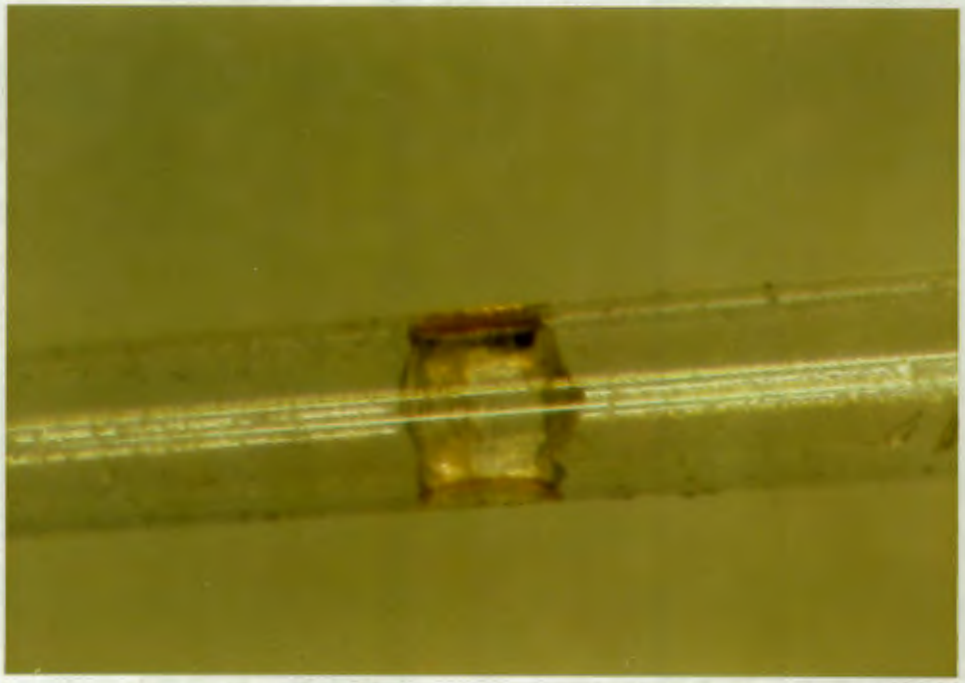

(b)

Figure 3.2 (a) Crystal of (III) mounted in a Lindemann capillary tube.
(b) Crystal of (IV) and mother liquor in a Lindemann tube.

Lattice Explorer for de Jong-Bouman, Buerger precession and cone-axis photographs. The appropriate cell dimensions obtained from preliminary crystal photography were confirmed by the diffraction data collections.

3.4.3. Intensity data-collections

Data-collections were carried out using an Enraf-Nonius CAD4 diffractometer with graphite-monochromated MoKα radiation (λ = 0.7107Å) generated by a Philips PW1730 model operating at 20mA, 50kV.

Accurate lattice parameters were obtained by least-squares analysis of 25 (compound (I)), or 24 (compounds (II), (III), (IV)), reflections measured in the range $16° < \theta < 17°$. The intensity data were collected in the ω - 2θ scan mode with variable scan speed* and a maximum recording time of 40s. During each data collection, three standard reflections were measured every 3600s to monitor the crystal stability and orientation control was performed every 200 reflections.

Lorentz-polarisation and absorption corrections were applied to all the data-collections. Further details of the data-collection parameters can be found in Tables 5.3, 5.6, 5.9 and 5.12 .

3.5. Computation

All computations, unless otherwise stated, were performed on a VAX/VMS (version 5.1-1) computer at the Computer Centre of the University of Cape Town.

The structures of compounds (I) to (III) were solved by direct methods and refined using SHELX-76 [64]. The structure of compound (IV) was solved by direct methods using SHELXS-86 [65] and refined using SHELX-76.

Molecular geometries including torsion angles [66], least-squares planes [67] and intermolecular contacts were calculated using PARST [68].

All packing diagrams and individual host-guest diagrams were drawn using PLUTO [69] from the PC version of "NRCVAX crystal structure system", running on an IBM/AT clone with VGA colour monitor, hard disk and mouse.

* Pre-scan speed $16.48° min^{-1}$

The various graphs were printed using HARVARD GRAPHICS [70] on the same IBM/AT as above.

CHAPTER FOUR

GUEST DESORPTION STUDIES

4. GUEST DESORPTION STUDIES

4.1. Introduction

The host structure as described by Toda *et al.* [54] is referred to as the α-phase. As mentioned in the introduction the molecular complex which crystallises from a solution of the host in guest is referred to as the β-phase. The aim of this set of experiments, and indeed one of the main aims of this project, was to desorb the guest molecules from crystals of each of the β-phases (compounds (I) - (IV)) to establish whether desorption occurs with or without retention of the crystalline host framework. In the former case, the product is referred to as the β_o-phase. In the latter case, the product is either the α-phase or a new species, designated the γ-phase (Figure 1.12).

The XRD pattern of the host alone as well as those of the four compounds before and after guest desorption were recorded (Figures 4.2 and 4.3). Comparison of these patterns enabled characterisation of the desorbed products according to the above scheme.

Guest desorption was achieved using the vacuum line, or, when this failed, a vacuum oven.

Calibration of the silica spring

The calibration of the spring (Table 4.1) was carried out at 18°C and at a pressure of approximately 2mmHg.

Figure 4.1 shows a plot of extension (mm) vs mass (mg).
The best straight line through the points was determined by least-squares and yielded a correlation coefficient of r = 0.9998, indicating excellent linearity over the range of measurement. From the slope we find the relation of extension to mass is 0.0581(3)mm/mg.

Table 4.1 Calibration of the silica spring

Cumulative Mass (mg)	Extension (mm)
58	3.3
96	5.8
147	8.8
198	12.0
233	13.9
245	14.6
303	18.0
355	21.0
414	24.5
478	28.1
542	31.8
642	37.2

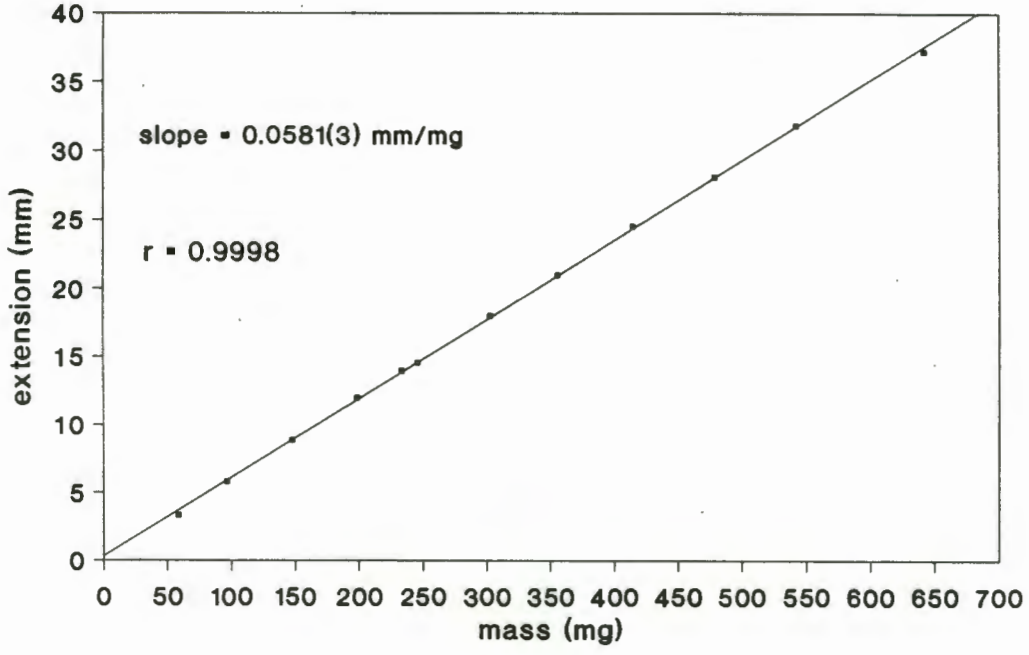

Figure 4.1 Calibration curve of the silica spring.

4.2. Guest loss results

4.2.1. Compound (I), $C_{26}H_{20}O_2 \cdot C_4H_8O$

A 0.583g (1.34mmol) sample of (I) was placed in the bucket and the system evacuated at 18°C. No change had occurred after one hour. On heating the water in the jacket surrounding the sample, no change was observed until a temperature of 68°C was reached. At this point, commencement of guest loss was indicated by slow contraction of the spring. After 90 minutes, no further contraction occurred, the system was allowed to cool to 18°C and the final position of the spring measured. An overall extension of 5.5(6)mm was obtained, corresponding to a mass loss of 95(4)mg. The calculated mass loss for complete guest desorption is 16.5% of 0.583g, or 96.2mg. The close agreement between the observed and the calculated figures indicated complete desorption of the guest.

The XRD patterns for compound (I) before and after guest desorption, (Figure 4.2) show considerable differences in peak positions and intensities. This result is not consistent with retention of the host framework after the loss of a small fraction of the scattering matter from crystals of host β-phase. In fact, except for a few discrepancies in intensity which could be attributed to preferred orientation effects, the XRD pattern of the desorbed product compares very favourably with that of the host alone (α-phase) and it is therefore concluded that upon guest desorption, the host framework collapses back to the α-phase.

4.2.2. Compounds (II), $C_{26}H_{20}O_2 \cdot 2C_7H_7N$ and (IV), $C_{26}H_{20}O_2 \cdot C_6H_7N$

A 0.271g (0.47mmol) sample of (II) was placed in the vacuum oven and the system evacuated at 85°C. The sample was reweighed after 90 minutes with the mass loss being 0.100g. The calculated mass loss for complete guest desorption is 36.6% of 0.271g, or 99mg and so complete guest desorption was assumed.

In the case of compound (IV) a 0.472g (1.03mmol) sample was placed in the vacuum oven and the system evacuated at 100°C. The sample showed a continual mass loss which slowed and eventually ceased after 7 hours. The mass loss was 0.098g. The calculated mass loss for complete guest desorption is 20.4% of 0.472g, or 96mg. Once again this indicated complete guest desorption.

Host = XRD pattern of guest-free host compound

β = XRD pattern before guest desorption

γ = XRD pattern after partial guest desorption

α = XRD pattern after total guest desorption

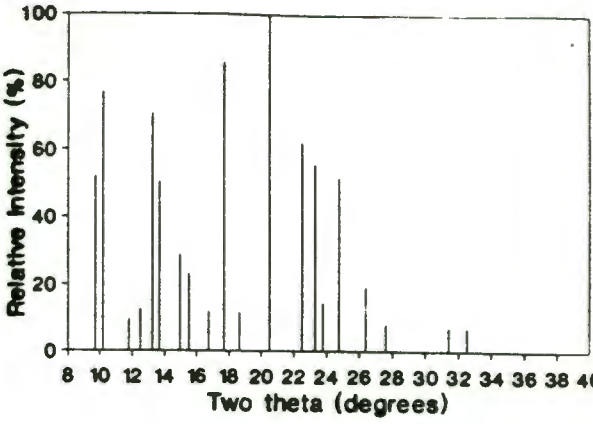

Host

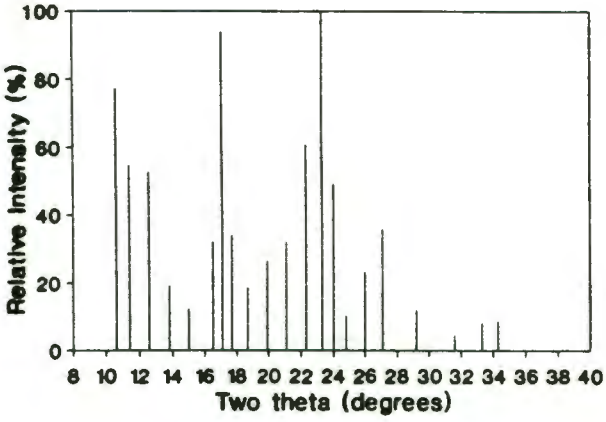

Compound (I) β- phase

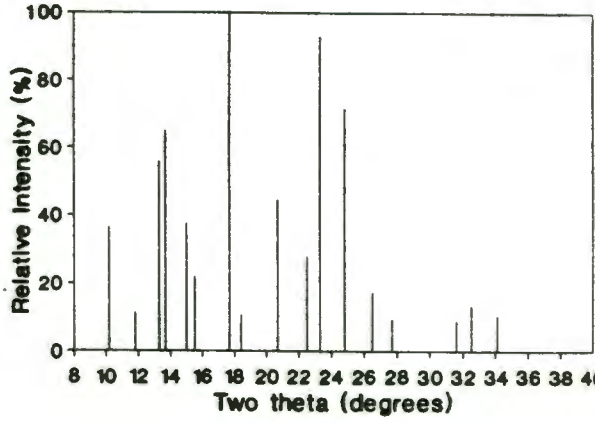

Compound (I) α- phase

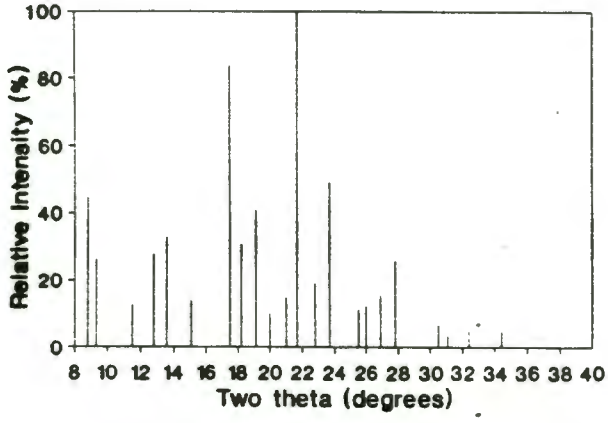

Compound (II) β- phase

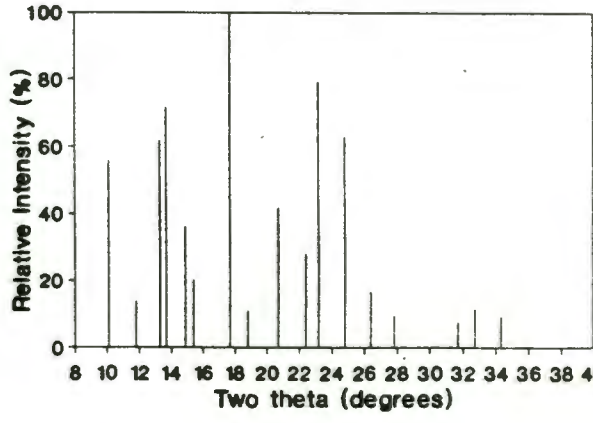

Compound (II) α- phase

Figure 4.2 X-ray powder diffraction patterns of guest desorption studies. Compounds (I) and (II).

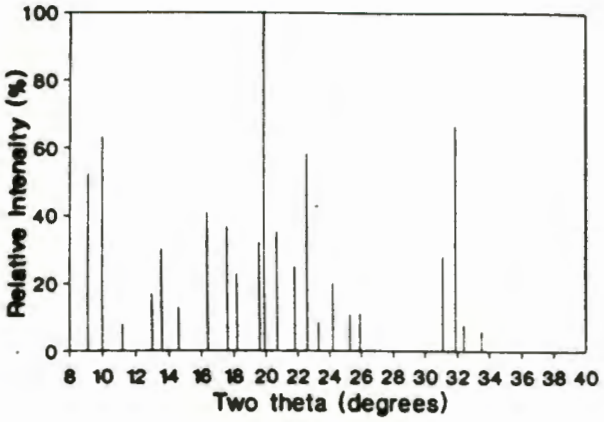

Compound (III) β- phase

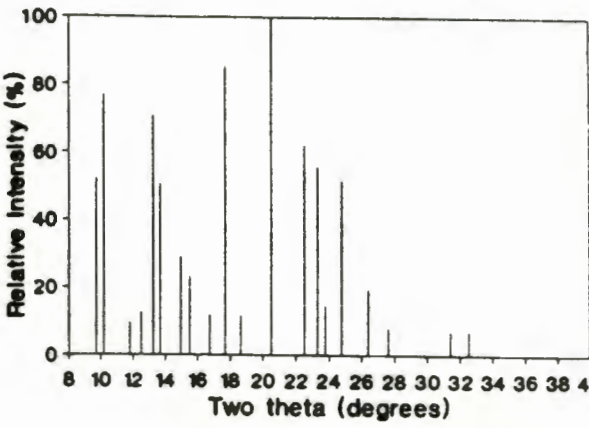

Host

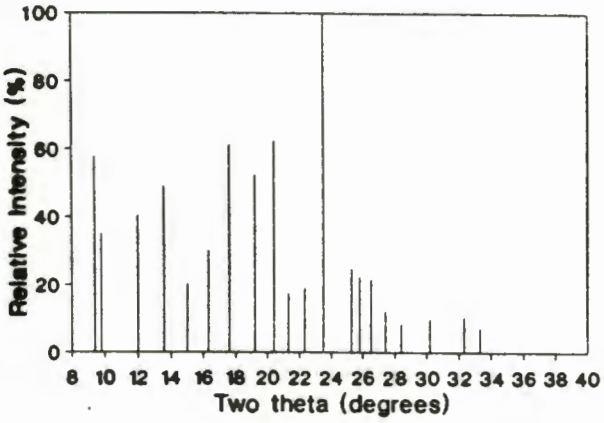

Compound (III) γ- phase

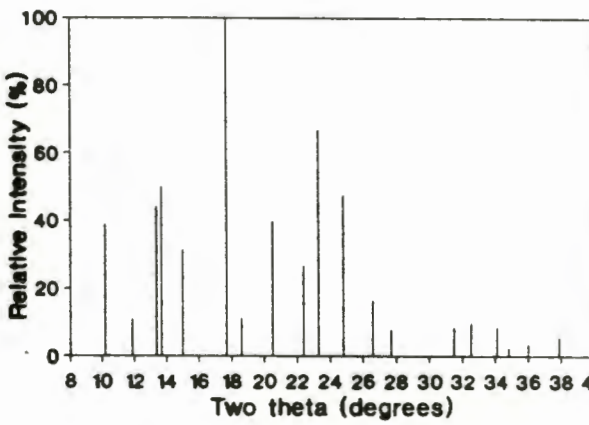

Compound (III) α- phase

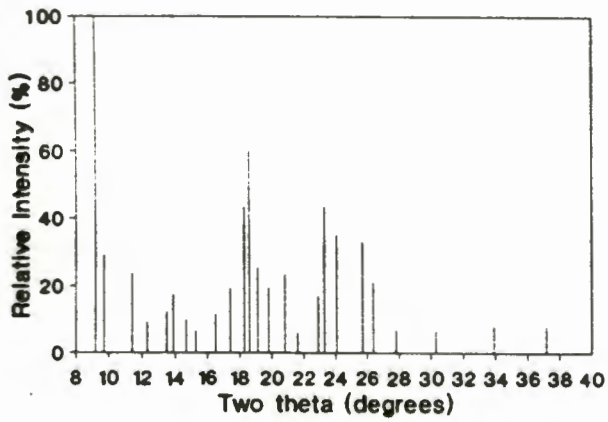

Compound (IV) β- phase

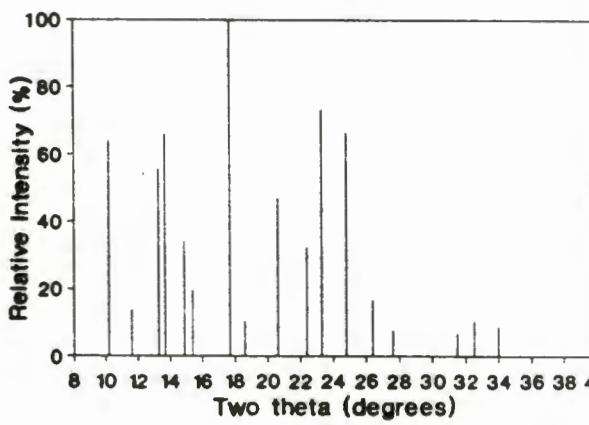

Compound (IV) α- phase

Figure 4.3 X-ray powder diffraction patterns of guest desorption studies. Compounds (III) and (IV).

As with compound (I), the XRD patterns for compounds (II) and (IV), before and after guest desorption, Figures 4.2 and 4.3 respectively, were considerably different, with the XRD patterns of the desorbed product comparing favourably with that of the host alone (α-phase). This again led to the conclusion that upon guest desorption the host framework collapses back to the α-phase.

4.2.3. Compound (III), $C_{26}H_{20}O_2 \cdot 2C_6H_7N$

Preliminary heating studies showed that compound (III) behaved differently from the other three compounds. This indicated the need for more careful control of the desorption process. The guest desorption was therefore carried out in a non-evacuated oven. A 0.270g (0.49mmol) sample of compound (III) was placed in the oven at 80°C. After 2 hours the sample weighed 0.219g consistent with a 19% mass loss. The calculated mass loss of one of the guests in this H:G 1:2 complex is 17% which indicates a guest loss of slightly more than 50% .

Complete guest desorption of compound (III) was achieved by placing a 0.510g (0.93mmol) sample in the oven at 130°C for 90 minutes. The mass loss on reweighing was 0.177g which represents 34.7% of the initial mass. The calculated mass loss for complete guest desorption is 33.6% of 0.510g, or 0.172g. The close agreement between observed and calculated figures for the mass loss indicated complete guest desorption.

The XRD patterns of compound (III) before, after partial, and after complete guest desorption (Figure 4.3) all show considerable differences in both peak positions and intensities. The pattern of the totally desorbed product compares very favourably with the host alone (α-phase) and once again it was concluded the host framework collapsed back to the α-phase upon total guest desorption. The pattern of the partially desorbed product did not compare closely with those of the starting material or the host alone. It was concluded that upon partial guest desorption the host molecular framework collapses to some γ-phase. Further guest desorption results in the γ-phase reverting to the α-phase.

4.3. Conclusion

Only guest desorption of compound (I) was achieved using the vacuum line as the temperature in the water jacket could not be raised above 70°C. Spring extension readings became more difficult as the increased water temperature decreased the visibility.

For all four compounds, the XRD patterns of the compounds after complete guest desorption compared very favourably in peak positions and intensities with that of the host alone. The only exception was the peak at $2\theta = 9.7°$ which only occurred as a shoulder in compound (IV) and was absent from the other three compounds. The similarity in the XRD patterns led to the conclusion that upon guest desorption the host framework collapses back to the α-phase. This phenomenon could later be explained by the fact that host-guest hydrogen-bonding occurs in all four compounds (see chapter 6) with the additional host-host hydrogen-bonding in compound (IV). Upon guest desorption the forces holding the β-framework together are lost when the host-guest hydrogen-bonds break and the host framework collapses back to the α-phase.

Compounds (II) and (III) have a host:guest ratio of 1:2. Compound (III) exhibits sequential guest loss (see section 7.2.) even though the two guests being centrosymmetrically related, are equivalent (see section 5.3.4.). This sequential guest loss could account for the intermediate γ-phase being formed upon partial guest desorption from compound (III). Preliminary experiments with 88% guest desorption from compound (III) gave an XRD pattern which resembled that of the γ-phase hence the γ-phase only collapses to the α-phase upon complete loss of the second guest. Compound (II) does not show this sequential guest loss (see section 7.2.) and in preliminary experiments the XRD pattern of a partially (36%) desorbed sample was the same as the β-phase.

CHAPTER FIVE

CHARACTERISATION AND STRUCTURE SOLUTION

5. CHARACTERISATION AND STRUCTURE SOLUTION

5.1. Density

The host to guest ratio can be determined using the measured density and the unit cell volume (taken from the diffractometer) in the following equation:-

$$Z_H M_H + Z_G M_G = D_m V N_A$$

(for details of the equation see Appendix 1)

Table 5.1 shows the measured density, calculated density and the host:guest ratio rounded off to the nearest integer. The measured density is usually lower than the calculated density due to small entrapped air bubbles.

The close agreement between the measured and calculated densities for the four compounds indicates that the actual host:guest ratio is very close to the rounded off host:guest ratio used in the calculated density equation. These host:guest ratios were supported by microanalyses (section 5.2.) and confirmed in the structure solutions (section 5.3.).

Table 5.1 Density measurements and Host:Guest ratios

Compound No.	D_m (g/cm^3)	D_c (g/cm^3)	H:G
(I)	1.248(4)	1.251	1:1
(II)	1.208(3)	1.219	1:2
(III)	1.226(3)	1.228	1:2
(IV)	1.271(4)	1.284	1:1

5.2. Microanalyses

Microanalysis of C, H, and N were performed on the four samples with the observed %O being derived from the difference between the C, H, N results and 100%. The calculated percentages were based on the host:guest ratios from Table 5.1 and the close agreement between observed and calculated values gives

further indication that these ratios are correct. This is later confirmed in the structure solution (section 5.3.).

Table 5.2 Microanalyses results.

	%C	%H	%N	%O
Compound (I)				
observed	82.3	6.4	-	11.3
calculated	82.5	6.5	-	11.0
Compound (II)				
observed	83.6	6.1	4.8	5.5
calculated	83.6	6.0	4.9	5.5
Compound (III)				
observed	82.9	6.4	5.0	5.7
calculated	82.9	6.2	5.1	5.8
Compound (IV)				
observed	83.9	6.2	3.0	6.9
calculated	84.0	5.9	3.1	7.0

5.3. Structure solution

5.3.1 Introduction

As stated in the experimental section 3.5., compounds (I) to (III) were solved using the SHELX-76 program [64]. For these compounds, normalised structure factors greater than 1.2 were used to produce convergence maps. The intensity statistics of these initial runs confirmed the centrosymmetry for compounds (I), (II) and (III). From the convergence maps, three origin defining reflections (satisfying the parity rules i.e. no reflection or linear combination of these reflections resulted in even, even, even parity) and around six multisolution reflections were chosen. The origin defining and multisolution reflections were chosen based on their high E and alpha (number of favourable interactions with other reflections) values as well as those reflections that were weak links in the phase propagation i.e. high

uncertainty in phase assignment. Using the Σ_2 relationship, the above reflections were used to generate phases and produce *E*-maps. The best eight maps were printed with the most probable chemical model being chosen. The non-hydrogen atoms of the host molecules were located, as were the guest atoms in compound (III) and their coordinates used as a trial model in the first difference Fourier map. Compound (IV) was solved using the program SHELXS-86's [65] automated structure solution as four attempts using different hand-selected starting sets of phases with SHELX-76 failed to produce a reasonable chemical model.

For all four compounds further refinement was achieved using SHELX-76. In subsequent difference Fourier maps the guest non-hydrogen atoms in compounds (I), (II) and (IV) and the majority of hydrogen atoms were located with all hydrogens but the hydroxy hydrogens being geometrically ideally placed in a riding model. The C-H distance was set at 1.08Å and common temperature factors (U_{iso}) values employed for each chemically distinct set. Full-matrix least-squares refinement on *F* (SHELX-76) involved minimisation of $\Sigma w(|F_o| - |F_c|)^2$ with $w = [\sigma^2(F_o) + g(F_o)^2]^{-1}$. The *g* value is chosen to ensure that $\Sigma w\Delta F^2$ did not show systematic variation with sinθ and with $(F_o/(F_o)_{max})^{½}$. Complex neutral atomic scattering factors for non-hydrogen atoms were taken from Cromer and Mann [71], and from Stewart, Davidson and Simpson [72] for hydrogen atoms. Dispersion corrections were taken from Cromer and Liberman [73]. Further details on the refinement of each compound can be found in the following sections. Observed and calculated structure factors as well as analyses of variance for all four structure solutions are listed on microfiche in Appendices 5. and 6. respectively. The host numbering scheme (Figure 5.1) will remain constant in all of the four compounds' structure solutions.

5.3.2. Compound (I), $C_{26}H_{20}O_2 \cdot C_4H_8O$

A total of 2183 reflections measured in the range indicated in table 5.3 yielded 1885 unique reflections. The data's internal consistency factor R_{int} (defined in Appendix 2) was 0.012 indicating good quality data before the structure was determined. The *E*-maps were produced using 319 reflections ($E(\text{min}) = 1.2$). The best *E*-map having the lowest R_A value (defined in Appendix 2) i.e. the best figure of merit, also revealed a chemically reasonable model from which the positions of all non-hydrogen host atoms were located. These atomic positions were used as a

trial model for the first difference Fourier map. The host atoms were centred around the Wyckoff special position (a), multiplicity of one in space group $P\bar{1}$. The refinement of these thermally isotropically treated atoms yielded an R value of 0.27 (R defined in Appendix 2 is the agreement between observed and calculated structure factors).

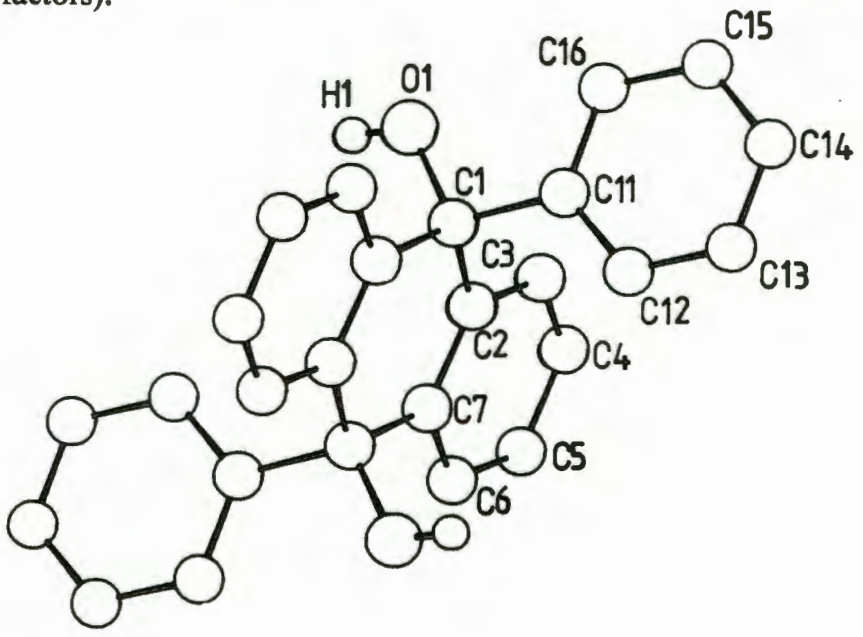

Figure 5.1 Host atomic numbering scheme. To simplify the picture only the hydroxy hydrogen is shown. The other hydrogen atoms are numbered according to the carbon to which they are bonded, e.g. H(3) is bonded to C(3)

In the resulting difference Fourier synthesis the majority of the host hydrogen atoms were located and fixed in a riding model, in geometrically placed, idealised positions. The temperature factors of the tricyclic ring hydrogens were linked as were those of the hydrogens attached to the host phenyl ring. The non-hydrogen atoms were treated anisotropically. Refinement of the modified input produced an R of 0.25 .

Once all the host atoms were identified in the solution model, three peaks stood out in the difference Fourier map having densities of between 3.63 and 2.76 $eÅ^{-3}$. These peaks were located around the Wyckoff special position (e), multiplicity of one. Using these three peaks the guest, 2-butanone could be modelled as a disordered molecule lying on a centre of symmetry. This is shown in Figure 5.2 . The two carbon atoms C(50) and C(60) as well as O(50) which is given a site

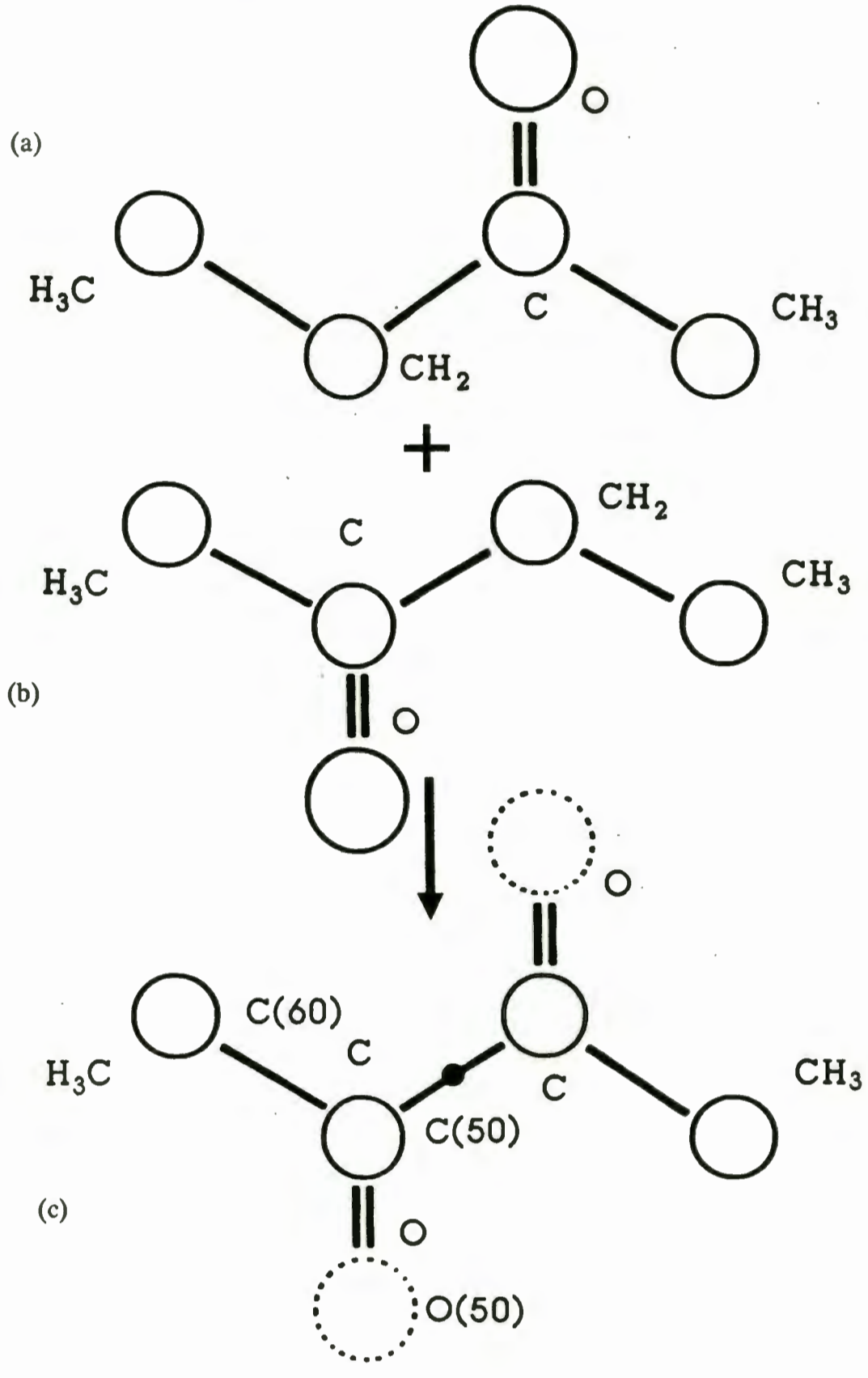

Figure 5.2 The two alternative disordered guest orientations ((a) and (b)) of 2-butanone. (c) is the guest modelling used in the structure solution. The oxygen atoms O(50) have a site occupancy of 0.5. The two alternative methylene hydrogens (also having half site occupancy) are not shown.

occupancy factor (s.o.f.) of 0.5 were placed in the structure model along with the host molecule. The refinement of the subsequent model yielded an R value of 0.094 indicating that the modelling of the guest disorder would appear to be correct.

All that remained was to locate the host hydroxy hydrogen, fix the guest methylene and methyl hydrogens, treat the guest non-hydrogen atoms anisotropically and set the weighting scheme. The hydroxy hydrogen was located from the difference Fourier map and allowed to refine freely. The methylene hydrogens were placed geometrically in an idealised riding model with s.o.f. of 0.5 and linked temperature factors. The methyl hydrogens were also geometrically placed in idealised positions but treated as a rigid group with common U_{iso} values.

The final least-squares refinement using 1690 observed reflections with $I_{rel}>2\sigma(I_{rel})$ yielded an R value of 0.059 . The g value in the weighting scheme was 0.026 and resulted in a weighted R_w (Appendix 2) value of 0.077 . The maximum (Δ/σ) value of 1.5 was associated with one of the parameters involved in rigid group refinement (zrot for C(60)) and the average (Δ/σ) of 0.001 show that the refinement had converged. The final non-hydrogen and hydroxy hydrogen coordinates are listed in Table 5.4 with the rest of the hydrogen atomic positions listed in Table 5.5 . All other data collection parameters and details of refinement can be found in Table 5.3 .

5.3.3. Compound (II), $C_{26}H_{20}O_2 \cdot 2C_7H_7N$

The X-ray data collection confirmed the space group $P2_1/c$ determined from preliminary photographs by exhibiting the non-extinction reflection conditions:

$$h0l \; : \; l=2n$$
$$0k0 \; : \; k=2n$$

A total of 3047 reflections were measured in the range shown in Table 5.6 with 38 systematic absences due to the above conditions. Of the total number of reflections measured 2292 were unique. The data collection quality was deemed to be good having a R_{int} of 0.017 . 404 reflections with normalised structure factors greater than 1.2 were used to generate eight E-maps. The E-map with the lowest

Table 5.3 Compound (I) Crystal data, experimental and refinement parameters.

Molecular formula	$C_{26}H_{20}O_2 \cdot C_4H_8O$
Molecular weight ($gmol^{-1}$)	436.55
Space group	$P\bar{1}$
a (Å)	7.924(1)
b (Å)	8.827(2)
c (Å)	9.050(1)
α (°)	109.93(2)
β (°)	97.31(1)
γ (°)	97.65(1)
Z	1
V ($Å^3$)	579.5(2)
D_c (gcm^{-3})	1.251
D_m (gcm^{-3}) (flotation in aq. KI)	1.248(4)
μ(MoKα) (cm^{-1})	0.74
F(000)	232

Data collection (21°C)

Crystal dimensions (mm)	.38 x .50 x .50
Range scanned θ (°)	$1 \leq \theta \leq 25$
Range of indices	$-9 \leq h \leq 9$, $-10 \leq k \leq 10$, $0 \leq l \leq 10$
Reflections for lattice parameters: no., θ range (°)	25, $16 \leq \theta \leq 17$
Indices of standard reflections	5 1 2, 2 4 3, 1 1 6
Intensity variation for standard reflections (%)	+2.4
Scan mode	$\omega - 2\theta$
Scan width in ω (°)	(0.85 + 0.35 tanθ)
Vertical aperture length (mm)	4
Aperture width (mm)	(1.12 + 1.05 tanθ)
Max. scan time (s)	40

Table 5.3 (cont.)

Number of reflections collected	2183
Number of unique reflections	1885
R_{int}	0.012
Number of reflections observed with $I_{rel} > 2\sigma(I_{rel})$	1690

Final refinement

Number of parameters	165
R	0.059
wR	0.077
w	$[\sigma^2(F_o) + 0.02609\, F_o^2]^{-1}$
S	0.689
Max. shift/e.s.d.	1.5
Average shift/e.s.d.	0.038
Max. height in difference Fourier map (e Å^{-3})	0.28
Min. height in difference Fourier map (e Å^{-3})	- 0.33
Absorption corrections: Min., Max., Average	0.9849, 0.9999, 0.9922

Table 5.4 Fractional atomic coordinates (x 10^4) and Thermal Parameters ($Å^2$ x 10^3) with e.s.d.'s in parentheses for Compound (I), $C_{28}H_{20}O_2 \cdot C_4H_8O$

Atom	x/a	y/b	z/c	Uiso/Uequiv(*)
C(1)	-64(2)	1567(2)	1382(2)	34(1) *
O(1)	1307(2)	2973(2)	2185(2)	48(1) *
H(1)	2306(47)	2879(46)	1949(47)	108(12)
C(2)	509(2)	73(2)	1620(2)	34(1) *
C(3)	1005(2)	164(3)	3193(2)	43(1) *
C(4)	1504(3)	-1150(3)	3511(2)	52(1) *
C(5)	1491(3)	-2587(3)	2255(3)	54(1) *
C(6)	1035(3)	-2689(2)	697(2)	46(1) *
C(7)	536(2)	-1362(2)	363(2)	35(1) *
C(11)	-1627(2)	1912(2)	2187(2)	34(1) *
C(12)	-3116(2)	712(2)	1712(2)	44(1) *
C(13)	-4537(3)	967(3)	2442(3)	53(1) *
C(14)	-4491(3)	2442(3)	3659(3)	56(1) *
C(15)	-3025(3)	3646(3)	4136(2)	57(1) *
C(16)	-1600(3)	3402(2)	3396(2)	46(1) *
C(50)	-4326(4)	-4243(5)	250(6)	102(2) *
O(50)†	-3778(6)	-3810(6)	-625(6)	100(2) *
C(60)	-3624(6)	-3375(5)	2056(5)	110(2) *

† s.o.f. = 0.5

Anisotropic atoms have thermal parameters ($Å^2$ x 10^3) of the form :

$$T = \exp\{-2\pi^2(U_{11}h^2a^{*2} + U_{22}k^2b^{*2} + U_{33}l^2c^{*2} + 2U_{23}klb^*c^* + 2U_{13}hla^*c^* + 2U_{12}hka^*b^*)\} \times 10^3,$$

with the following parameters :

Atom	U11	U22	U33	U23	U13	U12
C(1)	32(1)	34(1)	34(1)	12(1)	5(1)	1(1)
O(1)	42(1)	43(1)	50(1)	12(1)	2(1)	-6(1)
C(2)	27(1)	43(1)	34(1)	17(1)	8(1)	6(1)
C(3)	40(1)	62(1)	35(1)	23(1)	11(1)	15(1)
C(4)	49(1)	77(2)	45(1)	37(1)	14(1)	24(1)
C(5)	61(1)	68(1)	55(1)	40(1)	20(1)	30(1)
C(6)	54(1)	47(1)	48(1)	25(1)	17(1)	18(1)
C(7)	32(1)	39(1)	37(1)	18(1)	10(1)	6(1)
C(11)	38(1)	37(1)	30(1)	14(1)	6(1)	12(1)
C(12)	38(1)	47(1)	45(1)	13(1)	10(1)	7(1)
C(13)	38(1)	71(1)	53(1)	23(1)	12(1)	14(1)
C(14)	48(1)	83(2)	48(1)	28(1)	19(1)	33(1)
C(15)	74(2)	58(1)	43(1)	11(1)	18(1)	36(1)
C(16)	55(1)	42(1)	39(1)	9(1)	7(1)	12(1)
C(50)	84(2)	104(3)	171(4)	91(3)	72(3)	42(2)
O(50)	88(3)	114(4)	120(4)	70(3)	44(3)	-3(3)
C(60)	117(3)	106(3)	122(3)	56(2)	25(3)	30(2)

Table 5.5 Fractional atomic coordinates (x 10^4) for Compound (I), $C_{26}H_{20}O_2 \cdot C_4H_8O$

Parent atom	H	x/a	y/b	z/c
C(3)	H(3)	996	1280	4174
C(4)	H(4)	1902	-1056	4731
C(5)	H(5)	1840	-3634	2495
C(6)	H(6)	1064	-3806	-274
C(12)	H(12)	-3165	-441	756
C(13)	H(13)	-5680	13	2063
C(14)	H(14)	-5599	2649	4231
C(15)	H(15)	-2982	4793	5098
C(16)	H(16)	-472	4368	3759
C(50)	H(501)†	-5689	-4194	69
C(50)	H(502)†	-4173	-5504	-49
C(60)	H(601)	-4256	-4014	2723
C(60)	H(602)	-3865	-2137	2422
C(60)	H(603)	-2246	-3342	2288

† s.o.f. = 0.5

R_A value and 17 equivalent phase generated sets was found to be a chemically realistic model showing all host and guest non-hydrogen atoms. The host atoms were centred around the Wyckoff special position (d), multiplicity of two, with the guest 4-vinylpyridine in the general position *x,y,z*, multiplicity of four, thereby giving a host-guest ratio of 1:2 confirming the results found in sections 5.1. and 5.2. . These atomic positions were used as a trial model in the first difference Fourier map and resulted in an initial R of 0.15 .

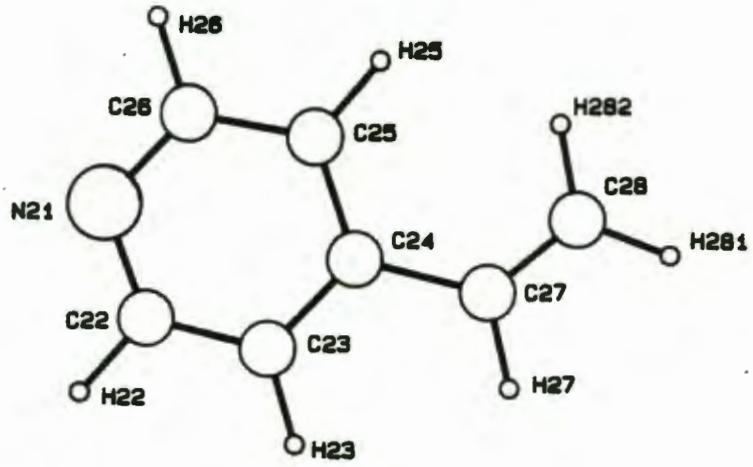

Figure 5.3 4-vinylpyridine numbering scheme (Compound (II)).

The non-hydrogen atoms of both host and guest were treated anisotropically and the aromatic hydrogens on both host and guest geometrically placed in idealised riding positions. The temperature factors of the tricyclic ring hydrogens were linked as were those of the phenyl hydrogens and guest aromatic hydrogens. The hydrogen bonded to C(27) (Figure 5.3) of the guest molecule was also located from the difference Fourier map and geometrically placed in an idealised riding position. The guest terminal methylene hydrogens were geometrically placed as a rigid group with linked temperature factors. The hydroxy hydrogen was located and allowed to refine without fixing constraints.

A number of least-squares cycles of refinement using 1655 observed reflections with $I_{rel}>2\sigma(I_{rel})$ saw the model converge as indicated by the max (Δ/σ) ratio of 0.11 with final agreement factor R = 0.054 and the weighted value R_w = 0.066 . Other data collection and structure refinement details of compound (II) can be

Table 5.6 Compound (II) Crystal data, experimental and refinement parameters.

Molecular formula	$C_{26}H_{20}O_2 \cdot 2C_7H_7N$
Molecular weight ($gmol^{-1}$)	574.72
Space group	$P2_1/c$
a (Å)	10.045(2)
b (Å)	18.630(3)
c (Å)	8.419(4)
α (°)	90
β (°)	96.29(3)
γ (°)	90
Z	2
V ($Å^3$)	1566.0(9)
D_c (gcm^{-3})	1.219
D_m (gcm^{-3}) (flotation in aq. KI)	1.208(3)
μ(MoKα) (cm^{-1})	0.70
F(000)	608

Data collection (21°C)

Crystal dimensions (mm)	.22 x .25 x .41
Range scanned θ (°)	$1 \leq \theta \leq 25$
Range of indices	$-11 \leq h \leq 11$
	$0 \leq k \leq 22$
	$0 \leq l \leq 10$
Reflections for lattice parameters: no., θ range (°)	24, $16 \leq \theta \leq 17$
Indices of standard reflections	7 5 2 , 4 11 3 , 2 3 6
Intensity variation for standard reflections (%)	+0.3
Scan mode	$\omega - 2\theta$
Scan width in ω (°)	(0.90 + 0.35 tanθ)
Vertical aperture length (mm)	4
Aperture width (mm)	(1.12 + 1.05 tanθ)
Max. scan time (s)	40

Table 5.6 (cont.)

Number of reflections collected	3047
Number of systematic absences	38
Number of unique reflections	2292
R_{int}	0.017
Number of reflections observed with $I_{rel} > 2\sigma(I_{rel})$	1655

Final refinement

Number of parameters	214
R	0.054
wR	0.066
w	$[\sigma^2(F_o) + 0.006467\, F_o^2]^{-1}$
S	0.759
Max. shift/e.s.d.	0.11
Average shift/e.s.d.	0.022
Max. height in difference Fourier map (e Å^{-3})	0.23
Min. height in difference Fourier map (e Å^{-3})	- 0.23
Absorption corrections: Min., Max., Average	0.9884, 0.9997, 0.9947

Table 5.7 Fractional atomic coordinates (x 10^4) and Thermal Parameters ($Å^2$ x 10^3) with e.s.d.'s in parentheses for Compound (II), $C_{26}H_{20}O_2 \cdot 2C_7H_7N$

Atom	x/a	y/b	z/c	Uiso/Uequiv(*)
C(1)	5030(3)	778(1)	5583(3)	42(1) *
O(1)	4624(2)	1412(1)	4700(3)	53(1) *
H(1)	4155(41)	1279(21)	3854(49)	73(12)
C(2)	3823(3)	285(2)	5658(3)	39(1) *
C(3)	2706(3)	567(2)	6258(4)	52(1) *
C(4)	1584(3)	150(2)	6395(4)	60(1) *
C(5)	1584(3)	-561(2)	5899(4)	59(1) *
C(6)	2676(3)	-842(2)	5296(4)	50(1) *
C(7)	3820(3)	-423(1)	5151(3)	40(1) *
C(11)	5543(3)	1020(1)	7277(3)	39(1) *
C(12)	5620(3)	1736(2)	7701(4)	48(1) *
C(13)	6102(4)	1936(2)	9241(4)	62(1) *
C(14)	6497(4)	1430(2)	10377(4)	62(1) *
C(15)	6419(3)	715(2)	9970(4)	62(1) *
C(16)	5940(3)	508(2)	8445(4)	51(1) *
N(21)	2726(3)	1257(2)	1962(4)	68(1) *
C(22)	1579(4)	900(2)	1789(5)	69(1) *
C(23)	577(3)	1020(2)	593(4)	63(1) *
C(24)	706(3)	1544(2)	-495(4)	56(1) *
C(25)	1905(4)	1921(2)	-376(4)	70(1) *
C(26)	2883(4)	1760(2)	885(5)	75(2) *
C(27)	-409(4)	1694(2)	-1768(5)	78(1) *
C(28)	-486(6)	2219(3)	-2714(7)	123(3) *

Anisotropic atoms have thermal parameters ($Å^2$ x 10^3) of the form :

$$T = \exp\{-2\pi^2(U_{11}h^2a^{*2} + U_{22}k^2b^{*2} + U_{33}l^2c^{*2} + 2U_{23}klb^*c^* + 2U_{13}hla^*c^* + 2U_{12}hka^*b^*)\} \times 10^3,$$

with the following parameters:

Atom	U11	U22	U33	U23	U13	U12
C(1)	41(2)	37(2)	45(2)	4(1)	-6(1)	2(1)
O(1)	58(1)	42(1)	54(1)	10(1)	-11(1)	3(1)
C(2)	37(2)	46(2)	33(1)	1(1)	-4(1)	2(1)
C(3)	40(2)	60(2)	53(2)	-4(2)	0(1)	5(1)
C(4)	40(2)	82(3)	57(2)	-3(2)	4(1)	5(2)
C(5)	39(2)	78(2)	60(2)	2(2)	4(2)	-11(2)
C(6)	44(2)	58(2)	47(2)	1(1)	-2(1)	-9(1)
C(7)	36(2)	45(2)	36(2)	2(1)	-4(1)	0(1)
C(11)	36(1)	39(1)	42(2)	0(1)	-1(1)	1(1)
C(12)	54(2)	41(2)	49(2)	-1(1)	4(1)	2(1)
C(13)	75(2)	53(2)	58(2)	-14(2)	8(2)	-5(2)
C(14)	68(2)	71(2)	45(2)	-11(2)	-1(2)	-9(2)
C(15)	63(2)	69(2)	49(2)	8(2)	-12(2)	-2(2)
C(16)	53(2)	45(2)	50(2)	5(1)	-10(1)	1(1)

Table 5.7 (cont.)

N(21)	57(2)	78(2)	66(2)	8(2)	-10(1)	6(2)
C(22)	63(2)	69(2)	74(3)	13(2)	2(2)	0(2)
C(23)	55(2)	63(2)	70(2)	2(2)	1(2)	-1(2)
C(24)	49(2)	64(2)	54(2)	-4(2)	-2(2)	5(2)
C(25)	71(2)	76(3)	62(2)	15(2)	6(2)	-2(2)
C(26)	53(2)	88(3)	81(3)	3(2)	-3(2)	-10(2)
C(27)	70(3)	87(3)	72(3)	7(2)	-11(2)	0(2)
C(28)	114(4)	130(4)	113(4)	50(4)	-46(3)	-17(3)

Table 5.8 Fractional atomic coordinates (x 10^4) for Compound (II), $C_{26}H_{20}O_2 \cdot 2C_7H_7N$

Parent atom	H	x/a	y/b	z/c
C(3)	H(3)	2710	1123	6628
C(4)	H(4)	722	373	6879
C(5)	H(5)	714	-893	5991
C(6)	H(6)	2663	-1398	4924
C(12)	H(12)	5303	2142	6826
C(13)	H(13)	6166	2498	9551
C(14)	H(14)	6865	1592	11576
C(15)	H(15)	6736	313	10855
C(16)	H(16)	5870	-55	8149
C(22)	H(22)	1427	488	2652
C(23)	H(23)	-321	697	513
C(25)	H(25)	2077	2330	-1239
C(26)	H(26)	3809	2059	986
C(27)	H(27)	-1230	1316	-1891
C(28)	H(281)	-1399	2309	-3491
C(28)	H(282)	242	2646	-2541

found in Table 5.6 and the final atomic positions in Tables 5.7 and 5.8 .

5.3.4. Compound (III), $C_{26}H_{20}O_2 \cdot 2C_6H_7N$

A total of 2764 reflections were measured in the range $1° \leq \theta \leq 25°$, as shown in Table 5.9 of which 2322 reflections were unique. The R_{int} value of 0.012 was indicative of a good quality data set. The generation of E-maps was achieved using 415 reflections with $E > 1.2$. The E-map with the lowest R_A value and the highest equivalent number of phase generated sets gave a realistic chemical model showing all host and guest non-hydrogen atoms. The first least-squares refinement using these atomic positions gave an initial R value of 0.13 .

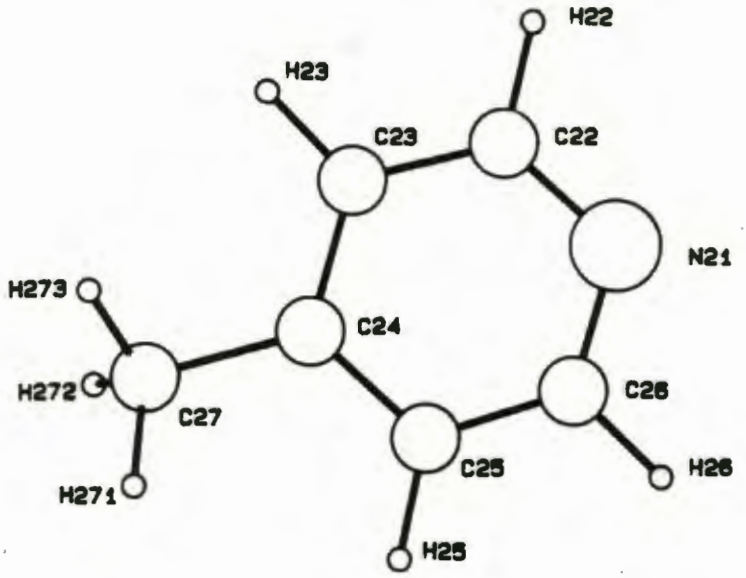

Figure 5.4 4-methylpyridine numbering scheme (Compound (III)).

The host atoms are centred around the Wyckoff special position (a) with a multiplicity of one and the guest 4-methylpyridine (4-picoline) is situated in the general position, x,y,z with a multiplicity of two in space group $P\bar{1}$. The host-guest ratio is therefore 1:2 confirming the ratio indicated in 5.1 and 5.2 .

From the first difference Fourier map, all host and guest hydrogen atoms were located. In subsequent least-squares refinements, all the host and guest aromatic

hydrogens were geometrically placed in idealised positions. The methyl hydrogens on the guest were geometrically placed in idealised positions but as a rigid model. The hydroxy hydrogen was allowed to refine without any constraints. All host and guest non-hydrogen atoms were allowed to refine anisotropically.

The model converged rapidly as shown by the average (Δ/σ) being 0.07 with the maximum (Δ/σ) value of 1.9 associated with one of the parameters involved in the rigid group refinement (zrot of C(27)) (Figure 5.4). The final R value using 1932 observed reflections with $I_{rel}>2\sigma(I_{rel})$ was 0.041 with R_w being 0.040 . The g value in the weighting scheme was left at zero as this gave constant analyses of variance. Final atomic positions of host and guest molecules in compound (III) can be found in Tables 5.10 and 5.11 .

5.3.5. Compound (IV), $C_{28}H_{20}O_2 \cdot C_6H_7N$

Of the total 5665 reflections collected, 3536 were unique. The R_{int} value of 0.023 showed the data set to be of good quality. Details of the data collection are contained in Table 5.12 . The structure was solved using SHELXS-86. The mean $|E^2-1|$ for the special reflections $0kl$, $h0l$, $hk0$ and the general reflections indicated the structure to be centrosymmetric.

160 subset reflections were selected on the basis of α_{est} with the 50 best subset phase permutations refined using a total of 398 reflections and a further four tangent refinement cycles. 2785 negative quartets [74] were found with 1000 being used in NQUAL, a figure of merit which approaches -1 for a more correct solution.

The best solution was extended by further tangent expansion. After one cycle of E-Fourier recycling, the point atom R-factor based on E-values, R_E, was 0.25 . From the highest 29 peaks, the non-hydrogen atoms of two host molecules were identified as well as a number of peaks approximating to a disordered guest.

The two host molecules' atomic positions located using SHELXS-86 were centred around the Wyckoff special position (c) and (g) in $P\bar{1}$. These atomic positions were used as a trial model in the first least-squares refinement using SHELX-76. The isotropically treated atoms yielded an R value of 0.29 .

Table 5.9 Compound (III) Crystal data, experimental and refinement parameters.

Molecular formula	$C_{26}H_{20}O_2 \cdot 2C_6H_7N$
Molecular weight ($gmol^{-1}$)	550.67
Space group	$P\bar{1}$
a (Å)	8.371(5)
b (Å)	9.599(2)
c (Å)	10.182(2)
α (°)	71.12(1)
β (°)	82.05(3)
γ (°)	74.45(3)
Z	1
V (Å^3)	744.6(5)
D_c (gcm^{-3})	1.228
D_m (gcm^{-3}) (flotation in aq. KI)	1.226(3)
μ(MoKα) (cm^{-1})	0.70
F(000)	292

Data collection (21°C)

Crystal dimensions (mm)	.16 x .19 x .50
Range scanned θ (°)	$1 \leq \theta \leq 25$
Range of indices	$-9 \leq h \leq 9$, $-11 \leq k \leq 11$, $0 \leq l \leq 12$
Reflections for lattice parameters: no., θ range (°)	24, $16 \leq \theta \leq 17$
Indices of standard reflections	2 2 8 , 4 7 4 , 5 6 4
Intensity variation for standard reflections (%)	+1.5
Scan mode	$\omega - 2\theta$
Scan width in ω (°)	(0.90 + 0.35 tanθ)
Vertical aperture length (mm)	4
Aperture width (mm)	(1.12 + 1.05 tanθ)
Max. scan time (s)	40

Table 5.9 (cont.)

Number of reflections collected	2764
Number of unique reflections	2322
R_{int}	0.012
Number of reflections observed with $I_{rel} > 2\sigma(I_{rel})$	1932

Final refinement

Number of parameters	201
R	0.041
wR	0.040
w	$[\sigma^2(F_o)]^{-1}$
S	2.525
Max. shift/e.s.d.	1.9
Average shift/e.s.d.	0.07
Max. height in difference Fourier map (e Å^{-3})	0.15
Min. height in difference Fourier map (e Å^{-3})	- 0.16
Absorption corrections: Min., Max., Average	0.9873, 0.9986, 0.9979

Table 5.10 Fractional atomic coordinates (x 10^4) and Thermal Parameters ($Å^2$ x 10^3) with e.s.d.'s in parentheses for Compound (III), $C_{26}H_{20}O_2 \cdot 2C_6H_7N$

Atom	x/a	y/b	z/c	Uiso/Uequiv(*)
C(1)	-66(2)	-1659(2)	390(2)	40(1) *
O(1)	1249(2)	-2921(2)	242(2)	53(1) *
H(1)	2136(35)	-2524(32)	-478(32)	143(12)
C(2)	428(2)	-971(2)	1377(2)	39(1) *
C(3)	851(2)	-1929(2)	2712(2)	50(1) *
C(4)	1280(3)	-1388(3)	3678(2)	58(1) *
C(5)	1303(3)	127(3)	3331(2)	58(1) *
C(6)	903(2)	1076(2)	2026(2)	51(1) *
C(7)	466(2)	541(2)	1031(2)	39(1) *
C(11)	-1588(2)	-2299(2)	1049(2)	41(1) *
C(12)	-1505(3)	-3835(2)	1485(2)	53(1) *
C(13)	-2906(3)	-4364(3)	2125(2)	67(1) *
C(14)	-4378(3)	-3362(3)	2298(2)	67(1) *
C(15)	-4476(3)	-1830(3)	1839(2)	62(1) *
C(16)	-3088(2)	-1293(2)	1222(2)	50(1) *
N(21)	3858(2)	7769(2)	8271(2)	58(1) *
C(22)	5279(3)	6775(3)	8680(2)	58(1) *
C(23)	6563(3)	6350(2)	7783(2)	55(1) *
C(24)	6409(3)	6984(2)	6373(2)	52(1) *
C(25)	4939(3)	8027(2)	5941(2)	59(1) *
C(26)	3726(3)	8373(3)	6905(3)	62(1) *
C(27)	7785(3)	6542(3)	5345(3)	87(1) *

Anisotropic atoms have thermal parameters ($Å^2$ x 10^3) of the form :

$$T = \exp\{-2\pi^2(U_{11}h^2a^{*2} + U_{22}k^2b^{*2} + U_{33}l^2c^{*2} + 2U_{23}klb^*c^* + 2U_{13}hla^*c^* + 2U_{12}hka^*b^*)\} \times 10^3,$$

with the following parameters :

Atom	U11	U22	U33	U23	U13	U12
C(1)	35(1)	39(1)	44(1)	-12(1)	3(1)	-6(1)
O(1)	43(1)	46(1)	61(1)	-15(1)	5(1)	0(1)
C(2)	27(1)	49(1)	40(1)	-11(1)	3(1)	-9(1)
C(3)	41(1)	57(1)	46(1)	-4(1)	-2(1)	-15(1)
C(4)	49(1)	82(2)	40(1)	-6(1)	-5(1)	-21(1)
C(5)	53(1)	81(2)	47(1)	-22(1)	-1(1)	-24(1)
C(6)	48(1)	60(1)	49(1)	-20(1)	0(1)	-17(1)
C(7)	29(1)	47(1)	41(1)	-14(1)	4(1)	-10(1)
C(11)	39(1)	45(1)	41(1)	-13(1)	0(1)	-13(1)
C(12)	53(1)	47(1)	61(1)	-12(1)	-3(1)	-17(1)
C(13)	79(2)	61(2)	68(2)	-10(1)	-4(1)	-39(1)
C(14)	59(2)	89(2)	65(2)	-21(1)	9(1)	-41(1)
C(15)	45(1)	81(2)	66(2)	-28(1)	10(1)	-22(1)

Table 5.10 (cont.)

C(16)	42(1)	53(1)	56(1)	-17(1)	6(1)	-14(1)
N(21)	53(1)	58(1)	62(1)	-20(1)	7(1)	-10(1)
C(22)	61(2)	65(2)	48(1)	-14(1)	-4(1)	-13(1)
C(23)	44(1)	59(1)	59(1)	-14(1)	-6(1)	-7(1)
C(24)	50(1)	57(1)	54(1)	-18(1)	4(1)	-19(1)
C(25)	59(1)	64(2)	49(1)	-7(1)	-4(1)	-12(1)
C(26)	51(1)	59(2)	66(2)	-9(1)	-7(1)	-2(1)
C(27)	68(2)	111(2)	76(2)	-37(2)	21(2)	-12(2)

Table 5.11 Fractional atomic coordinates (x 10^4) for Compound (III), $C_{26}H_{20}O_2 \cdot 2C_6H_7N$

Parent atom	H	x/a	y/b	z/c
C(3)	H(3)	842	-3112	2985
C(4)	H(4)	1599	-2140	4702
C(5)	H(5)	1634	559	4084
C(6)	H(6)	926	2255	1762
C(12)	H(12)	-359	-4626	1332
C(13)	H(13)	-2832	-5567	2485
C(14)	H(14)	-5457	-3778	2794
C(15)	H(15)	-5638	-1043	1961
C(16)	H(16)	-3171	-88	872
C(22)	H(22)	5434	6272	9782
C(23)	H(23)	7681	5526	8182
C(25)	H(25)	4753	8564	4846
C(26)	H(26)	2588	9187	6537
C(27)	H(271)	7741	7495	4415
C(27)	H(272)	7760	5551	5072
C(27)	H(273)	8914	6329	5854

The 2-methylpyridine (2-picoline) guest molecules appeared to be disordered and in the general position, *x,y,z*, hence the host:guest ratio of 1:1. The disorder shown in Figure 5.5 shows the two alternative guest positions which are coplanar and related by an approximate mirror plane perpendicular to their mean plane. Each of the two rings was fixed in a hexagonal conformation (although a pyridine ring is not exactly hexagonal, it is a good approximation). The peak heights of the two alternative ring positions in the difference Fourier map were similar and the atoms of the two rings were all given s.o.f.'s of 0.5 . All the guest non-hydrogen atoms' temperature factors were linked. The resulting refinement realised an *R* value of 0.13 .

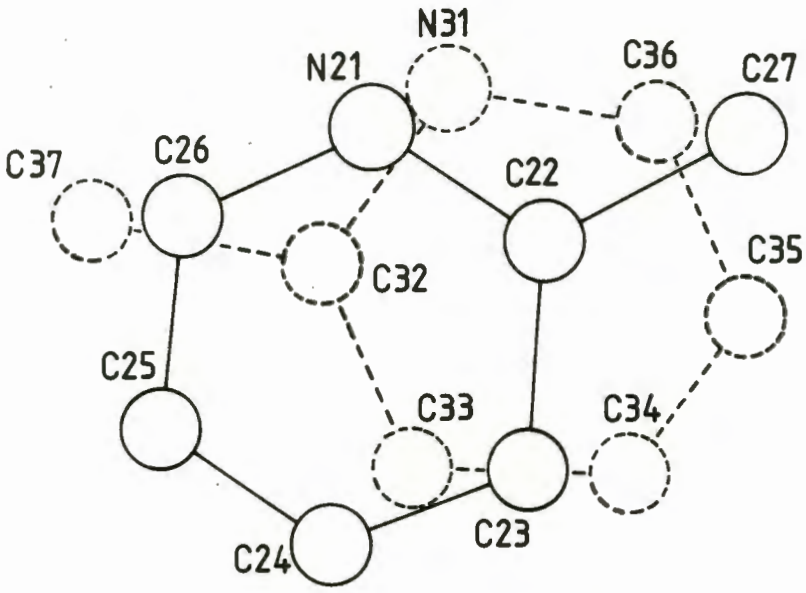

Figure 5.5 The two alternative orientations found for the guest 2-methylpyridine in Compound (IV).

The two guest s.o.f.'s were allowed to vary with their sum adding to unity. The hexagonal ring constraints were relaxed giving reasonable bond lengths and angles. The hydrogen positions for all but the hydroxy hydrogens were geometrically placed in idealised positions as a riding model, with chemically similar hydrogens having their temperature factors linked. The hydroxy hydrogens on both host molecules were located from the difference Fourier maps and allowed to refine without restrictions. The non-hydrogen atoms of the two host molecules were

treated anisotropically whereas the guest non-hydrogen atoms were refined isotropically.

The final least-squares refinement showed the population parameters of the two guest positions in the ratio 0.55:0.45 for the N(21)- and N(31)- containing rings respectively. The final least-squares refinement using 2530 observed reflections with $I_{rel} > 2\sigma(I_{rel})$ yielded a R value of 0.060 with the R_w value being 0.065 . The maximum (Δ/σ) value was 0.17 and an average value of 0.001 showing that the refinement had converged. The final atomic coordinates are listed in Tables 5.13 and 5.14 with the reported coordinates for the two alternative guest orientations related through the inversion centre at 0,0,0 .

Table 5.12 Compound (IV) Crystal data, experimental and refinement parameters.

Molecular formula	$C_{26}H_{20}O_2 \cdot C_6H_7N$
Molecular weight ($gmol^{-1}$)	457.57
Space group	$P\bar{1}$
a (Å)	9.337(2)
b (Å)	10.407(3)
c (Å)	13.470(9)
α (°)	70.75(3)
β (°)	87.65(3)
γ (°)	73.58(2)
Z	2
V ($Å^3$)	1183.2(9)
D_c (gcm^{-3})	1.284
D_m (gcm^{-3}) (flotation in aq. KI)	1.271(4)
$\mu(MoK_\alpha)$ (cm^{-1})	0.74
F(000)	484

Data collection (21°C)

Crystal dimensions (mm)	.34 x .38 x .38
Range scanned θ (°)	$1 \leq \theta \leq 25$
Range of indices	$-11 \leq h \leq 11$, $-12 \leq k \leq 12$, $0 \leq l \leq 16$
Reflections for lattice parameters: no., θ range (°)	24, $16 \leq \theta \leq 17$
Indices of standard reflections	4 8 2 , 3 6 9 , -6 3 1
Intensity variation for standard reflections (%)	- 10.5
Scan mode	ω - 2θ
Scan width in $\overset{\omega}{\wedge}$(°)	(0.85 + 0.35 tanθ)
Vertical aperture length (mm)	4
Aperture width (mm)	(1.20 + 1.45 tanθ)
Max. scan time (s)	40

Table 5.12 (cont.)

Number of reflections collected	5665
Number of unique reflections	3536
R_{int}	0.023
Number of reflections observed with $I_{rel} > 2\sigma(I_{rel})$	2530
Final refinement	
Number of parameters	330
R	0.060
wR	0.065
w	$[\sigma^2(F_o) + 0.00554\, F_o^2]^{-1}$
S	1.994
Max. shift/e.s.d.	0.17
Average shift/e.s.d.	0.001
Max. height in difference Fourier map (e Å^{-3})	0.28
Min. height in difference Fourier map (e Å^{-3})	- 0.26
Absorption corrections: Min., Max., Average	0.8680, 0.9896, 0.8955

Table 5.13 Fractional atomic coordinates (x 10^4) and Thermal Parameters ($Å^2$ x 10^3) with e.s.d. s in parentheses for Compound (IV), $C_{26}H_{20}O_2 \cdot C_6H_7N$

Atom	x/a	y/b	z/c	Uiso/Uequiv(*)
C(1)	566(3)	6192(3)	9257(2)	38(1) *
O(1)	731(2)	6463(2)	8144(2)	47(1) *
H(1)	483(42)	5704(43)	7920(31)	86(13)
C(2)	-1076(3)	6359(3)	9474(2)	35(1) *
C(3)	-2110(3)	7668(3)	8962(3)	45(1) *
C(4)	-3617(3)	7878(4)	9106(3)	53(2) *
C(5)	-4129(3)	6788(3)	9763(3)	51(2) *
C(6)	-3119(3)	5495(3)	10269(3)	45(1) *
C(7)	-1587(3)	5259(3)	10139(2)	37(1) *
C(11)	1074(3)	7336(3)	9516(2)	38(1) *
C(12)	1152(4)	7289(4)	10554(3)	48(2) *
C(13)	1659(4)	8268(4)	10802(3)	58(2) *
C(14)	2095(4)	9317(4)	10032(4)	61(2) *
C(15)	2007(4)	9377(3)	9001(3)	60(2) *
C(16)	1490(3)	8395(3)	8743(3)	48(1) *
C(1B)	671(3)	4558(3)	6127(2)	36(1) *
O(1B)	-72(2)	4795(2)	7034(2)	43(1) *
H(1B)	-1029(57)	5350(52)	6857(40)	125(19)
C(2B)	-19(3)	3638(3)	5737(2)	36(1) *
C(3B)	-43(3)	2319(3)	6454(3)	48(1) *
C(4B)	-607(4)	1399(3)	6161(3)	54(2) *
C(5B)	-1164(4)	1784(4)	5136(3)	52(2) *
C(6B)	-1173(3)	3085(3)	4424(3)	45(1) *
C(7B)	-601(3)	4025(3)	4711(2)	35(1) *
C(11B)	2299(3)	3732(3)	6500(2)	38(1) *
C(12B)	3359(3)	3652(4)	5745(3)	57(2) *
C(13B)	4829(4)	2856(5)	6050(4)	73(2) *
C(14B)	5258(4)	2135(4)	7109(4)	70(2) *
C(15B)	4220(4)	2233(4)	7853(3)	60(2) *
C(16B)	2745(3)	3031(3)	7555(3)	45(1) *
N(21)†	2909(7)	3157(8)	3374(5)	48(2)
C(22)†	4193(7)	3400(7)	3073(5)	54(2)
C(23)†	5511(12)	2195(10)	3179(7)	67(2)
C(24)†	5268(10)	907(12)	3569(7)	75(3)
C(25)†	3965(10)	681(9)	3846(7)	85(3)
C(26)†	2772(11)	1832(10)	3754(7)	73(3)
C(27)†	4260(13)	4866(12)	2645(9)	96(4)
N(31)‡	-2927(7)	-3694(9)	-3191(5)	44(2)
C(32)‡	-3547(9)	-2254(9)	-3514(6)	47(2)
C(33)‡	-5104(11)	-1662(14)	-3441(8)	59(3)
C(34)‡	-5912(12)	-2643(11)	-3054(8)	66(3)
C(35)‡	-5373(10)	-3958(10)	-2809(7)	68(3)
C(36)‡	-3882(11)	-4510(12)	-2843(8)	65(3)
C(37)‡	-2470(12)	-1395(12)	-3916(9)	73(4)

† s.o.f. = 0.55
‡ s.o.f. = 0.45

Table 5.13 (cont.)

Anisotropic atoms have thermal parameters ($Å^2 \times 10^3$) of the form :

$$T = \exp\{-2\pi^2(U_{11}h^2a^{*2} + U_{22}k^2b^{*2} + U_{33}l^2c^{*2} + 2U_{23}klb^*c^* + 2U_{13}hla^*c^* + 2U_{12}hka^*b^*)\} \times 10^3,$$

with the following parameters :

Atom	U11	U22	U33	U23	U13	U12
C(1)	42(2)	42(2)	35(2)	-16(1)	2(1)	-14(1)
O(1)	57(1)	57(1)	37(1)	-20(1)	5(1)	-22(1)
C(2)	35(2)	38(2)	37(2)	-16(1)	-1(1)	-9(1)
C(3)	44(2)	44(2)	49(2)	-16(2)	-5(2)	-10(2)
C(4)	41(2)	48(2)	70(3)	-25(2)	-10(2)	0(2)
C(5)	32(2)	55(2)	71(3)	-31(2)	0(2)	-7(2)
C(6)	34(2)	49(2)	58(2)	-23(2)	5(1)	-11(1)
C(7)	32(2)	42(2)	43(2)	-20(1)	0(1)	-10(1)
C(11)	31(2)	39(2)	46(2)	-15(1)	4(1)	-10(1)
C(12)	48(2)	60(2)	46(2)	-25(2)	4(2)	-22(2)
C(13)	51(2)	72(3)	66(3)	-39(2)	2(2)	-19(2)
C(14)	43(2)	52(2)	100(3)	-40(2)	-4(2)	-11(2)
C(15)	49(2)	39(2)	88(3)	-13(2)	-1(2)	-15(2)
C(16)	46(2)	39(2)	54(2)	-10(2)	1(2)	-11(1)
C(1B)	34(2)	45(2)	31(2)	-14(1)	3(1)	-11(1)
O(1B)	41(1)	56(1)	34(1)	-17(1)	5(1)	-12(1)
C(2B)	30(2)	40(2)	40(2)	-12(1)	5(1)	-11(1)
C(3B)	49(2)	48(2)	46(2)	-8(2)	-2(2)	-19(2)
C(4B)	58(2)	47(2)	57(2)	-7(2)	1(2)	-25(2)
C(5B)	55(2)	54(2)	60(2)	-24(2)	6(2)	-26(2)
C(6B)	50(2)	55(2)	42(2)	-18(2)	5(2)	-26(2)
C(7B)	30(1)	44(2)	35(2)	-15(1)	4(1)	-12(1)
C(11B)	35(2)	43(2)	40(2)	-15(1)	-1(1)	-12(1)
C(12B)	38(2)	83(3)	51(2)	-29(2)	3(2)	-9(2)
C(13B)	40(2)	105(3)	75(3)	-41(3)	4(2)	-7(2)
C(14B)	38(2)	89(3)	84(3)	-39(2)	-12(2)	0(2)
C(15B)	53(2)	66(2)	57(2)	-21(2)	-16(2)	-6(2)
C(16B)	45(2)	46(2)	42(2)	-12(2)	-4(1)	-10(1)

Table 5.14 Fractional atomic coordinates (x 10^4) for Compound (IV), $C_{26}H_{20}O_2 \cdot C_6H_7N$

Parent atom	H	x/a	y/b	z/c
C(3)	H(3)	-1720	8528	8449
C(4)	H(4)	-4399	8896	8703
C(5)	H(5)	-5310	6947	9878
C(6)	H(6)	-3520	4642	10781
C(12)	H(12)	818	6475	11169
C(13)	H(13)	1711	8220	11614
C(14)	H(14)	2502	10078	10235
C(15)	H(15)	2343	10192	8388
C(16)	H(16)	1412	8460	7929
C(3B)	H(3B)	392	2013	7253
C(4B)	H(4B)	-615	386	6728
C(5B)	H(5B)	-1590	1064	4895
C(6B)	H(6B)	-1630	3387	3629
C(12B)	H(12B)	3032	4208	4920
C(13B)	H(13B)	5644	2798	5462
C(14B)	H(14B)	6401	1500	7346
C(15B)	H(15B)	4554	1685	8677
C(16B)	H(16B)	1941	3104	8148
C(23)	H(23)†	6599	2325	2953
C(24)	H(24)†	6218	-13	3669
C(25)	H(25)†	3853	-383	4133
C(26)	H(26)†	1699	1674	3994
C(271)	H(271)†	5389	4871	2439
C(272)	H(272)†	3940	5367	3239
C(273)	H(273)†	3508	5444	1954
C(33)	H(33)‡	-5623	-531	-3671
C(34)	H(34)‡	-7092	-2229	-2970
C(35)	H(35)‡	-6096	-4641	-2566
C(36)	H(36)‡	-3419	-5650	-2587
C(371)	H(371)‡	-3060	-278	-4151
C(372)	H(372)‡	-1937	-1641	-4584
C(373)	H(373)‡	-1631	-1653	-3298

† s.o.f. = 0.55
‡ s.o.f. = 0.45

CHAPTER SIX

DISCUSSION OF STRUCTURES

6. DISCUSSION OF STRUCTURES

6.1. Host conformation

The conformation of the host compound, *trans*-9,10-dihydroxy-9,10-diphenyl-9,10-dihydroanthracene is very similar in all four of the structures. The host molecules in compounds (I) to (IV) all occupy centrosymmetric sites. The *trans* orientation of the two phenyl and two hydroxy central ring substituents satisfies the symmetry requirement.

The conformational preference of the central 1,4-cyclohexadiene ring (planar or folded) in 9,10-substituted-9,10-dihydroanthracene compounds depends on the degree of ~~stereochemistry~~ substitution as well as on the steric bulk of the substituents [54,75]. Asymmetry parameters ΔC_S and ΔC_2 are used as a measure of ring deviation from ideal symmetry and are calculated from torsion angles [76]. The equations used in the calculation of these values are given in Appendix 1. In all four compounds the endocyclic torsion angles in the host central 1,4-cyclohexadiene rings are all less than 3°, yielding asymmetry parameters ΔC_S and ΔC_2 less than 0.3 . These low values indicate the central ring to be essentially planar as are all but one [76,48] of those previously reported in studies of *trans*-9,10-dihydroxy-9,10-diphenyl-9,10-dihydroanthracene.

As the maximum out-of-plane deviation of any C atom from the fused aromatic ring is only 0.006(2)Å, the entire tricyclic system is effectively planar in all four compounds. The maximum out-of-plane deviation of the phenyl moieties is 0.010(2)Å. Dihedral angles between the planes of the tricyclic systems and the phenyl substituents are in the range 84.3(1) to 89.1(1)°. Tables of least-squares planes are listed on microfiche in Appendix 4.

The final bond lengths, bond angles, and torsion angles for compounds (I) to (IV) are on microfiche in Appendix 3.

Bond lengths and bond angles for all four compounds, are in close agreement and also compare well with those reported for structures containing *trans*-9,10-dihydroxy-9,10-diphenyl-9,10-dihydroanthracene [54-56]. For all four compounds no bond length differed by more than 0.02Å and no bond angle deviated by more

than 2.5° from that of the host's guest-free structure [54], these minor discrepancies being due to vibrational effects and not different bonding schemes.

6.2. Crystal structures and molecular packing

6.2.1. Compound (I), $C_{26}H_{20}O_2 \cdot C_4H_8O$

Atomic numbering for compound (I) is shown in Figure 6.1. To satisfy the space group requirements of $P\bar{1}$ one host molecule can be located at a centre of symmetry and the unsymmetrical 2-butanone molecule disordered over two related general sites or at a second symmetry centre. As indicated in section 5.3.2., the 2-butanone was modelled at a centre of symmetry with the C(50)-C(50^i) bond length (bonding between C(50) and its centrosymmetric counterpart) of 1.489(5)Å. This is only nominally significantly different from the standard C-C bond shortened in the presence of a C=O bond having a value of 1.511(15) [77]. The significance expression is given in Appendix 1. The C=O bond of 1.101(8)Å is significantly different from the standard C=O bond of 1.210(8) and is attributed to the guest disorder.

The stereoscopic molecular packing diagram depicted in Figure 6.2 suggests that the guest molecules occupy channels parallel to [001], and that each guest carbonyl oxygen atom is hydrogen bonded to the host hydroxy function (shown by the dotted lines). The O(1)$\cdots$O(50) distance of 2.721(6)Å and O(1)-H(1)$\cdots$O(50) bond angle of 134(4)° meet the requirements of hydrogen-bonding. The requirement of hydrogen-bonding is that the distance between atoms must be less than the sum of the van der Waals radii (the latter taken from Bondi [78]). No other hydrogen bonds were found to exist. Table 6.1 shows hydrogen bond details for all four compounds.

The 1:1 host:guest ratio exhibited in this compound is in contrast to recent structural studies of molecular inclusion complexes of the same host with the ketones: acetophenone, 3-methylcyclopentanone, 2- and 4-methylcyclopentanone [55,56]. These studies show a 1:2 host:guest ratio as the norm, with the host molecule located at a centre of symmetry hydrogen bonded (-OH$\cdots$O=C) to two ketone molecules situated in general positions.

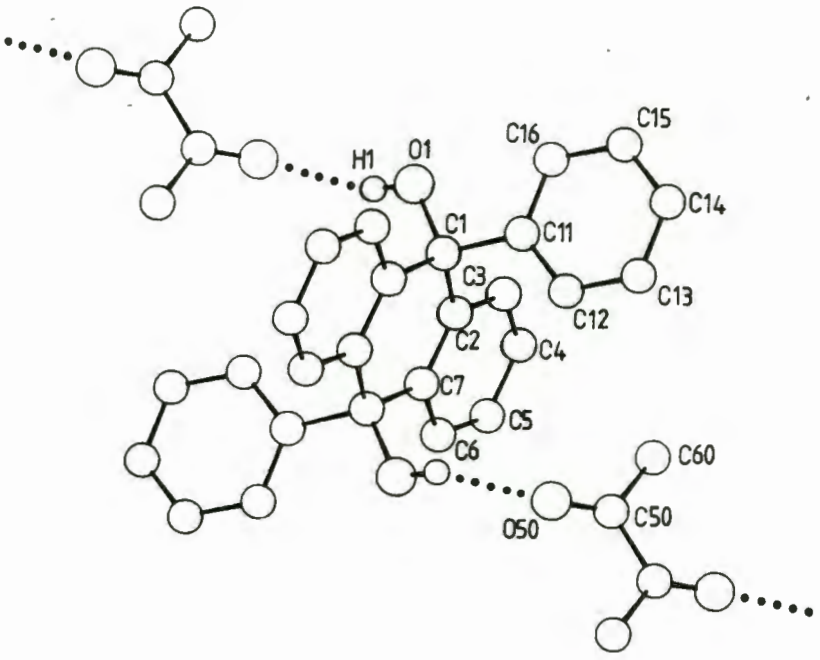

Figure 6.1 Perspective view of Compound (I). For clarity only the hydroxy hydrogen is shown. Dotted lines indicate hydrogen bonds.

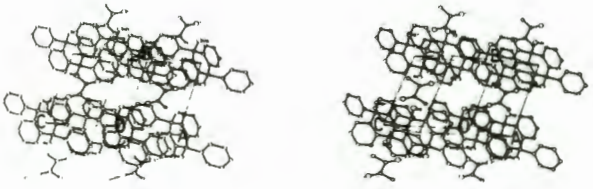

Figure 6.2 Stereoview of molecular packing in Compound (I). For clarity only the hydroxy hydrogen is shown. Hydrogen bonds are indicated by dotted lines.

Table 6.1 Hydrogen-bonding details of compounds (I) to (IV)

Compound	Donor-H/Å	Donor····Acceptor/Å	H····Acceptor/Å	Donor-H····Acceptor/°
(I)	O(1)-H(1) 0.85(4)	O(1)····O(50^{i}) 2.721(6)	H(1)····O(50^{i}) 2.06(5)	O(1)-H(1)····O(50^{i}) 134(4)
(II)	O(1)-H(1) 0.87(4)	O(1)····N(21^{ii}) 2.841(4)	H(1)····N(21^{ii}) 2.00(4)	O(1)-H(1)····N(21^{ii}) 163(4)
(III)	O(1)-H(1) 1.03(3)	O(1)····N(21^{iii}) 2.817(3)	H(1)····N(21^{iii}) 1.81(3)	O(1)-H(1)····N(21^{iii}) 168(3)
(IV)	O(1)-H(1) 1.02(5)	O(1)····O(1B^{iv}) 2.892(4)	H(1)····O(1B^{iv}) 1.91(5)	O(1)-H(1)····O(1B^{iv}) 160(4)
	O(1B)-H(1B) 0.91(5)	O(1B)····N(21^{v}) 2.831(6)	H(1B)····N(21^{v}) 1.94(5)	O(1B)-H(1B)····N(21^{v}) 166(5)
	O(1B)-H(1B) 0.91(5)	O(1B)····N(31^{vi}) 2.656(6)	H(1B)····N(31^{vi}) 1.76(5)	O(1B)-H(1B)····N(31^{vi}) 168(5)

(i) -x, -y, -z
(ii) x, y, z
(iii) x, y-1, z-1
(iv) x, y, z
(v) -x, 1-y, 1-z
(vi) x, 1+y, 1+z

6.2.2. Compound (II), $C_{26}H_{20}O_2 \cdot 2C_7H_7N$

The atomic numbering for compound (II) is shown in Figure 6.3 . The space group requires that this compound with a 1:2 host:guest ratio, has the host molecule located at a centre of symmetry with the guest molecule occupying a general position. By this arrangement the host molecule is associated with two guest molecules by O-H$\cdots$N hydrogen bonds (Table 6.1). In this respect compound (II) is a structural analogue of the 1:2 ketone complexes discussed at the end of the preceding section. The O(1)$\cdots$N(21) distance of 2.841(4)Å and O(1)-H(1)$\cdots$N(21) angle of 163(4)° satisfies hydrogen bond requirements.

The guest pyridine is essentially planar with C(24) having the maximum out-of-plane deviation of 0.014(4)Å. The dihedral angle between the pyridine ring and the plane through C(24), C(27) and C(28) is 10.2(4)°. The dihedral angle between the host phenyl ring and the substituted pyridine ring is 55.0(1)°. The stereoscopic molecular packing diagram of (II) depicted in Figure 6.4 shows that there is no evidence of parallel stacking of the substituted pyridine molecules either with themselves or with the host phenyl rings. This leaves the O-H$\cdots$N hydrogen bonds and the general van der Waals contacts as the only sources of cohesion in the crystal of compound (II).

6.2.3. Compound (III), $C_{26}H_{20}O_2 \cdot 2C_6H_7N$

Compound (III), having a 1:2 host:guest ratio, is structurally similar to (II) even though (III) crystallizes in space group $P\bar{1}$ as opposed to $P2_1/c$. Figure 6.5 shows the atomic numbering of (III). The host molecule located at a centre of symmetry is O-H$\cdots$N hydrogen bonded to two guest molecules situated in general positions. The conditions for hydrogen bonding (Table 6.1) are satisfied by a O(1)$\cdots$N(21) bond length of 2.817(3)Å and O(1)-H(1)$\cdots$N(21) angle of 168(3)°.

The substituted pyridine ring has a maximum out-of-plane deviation of 0.005(3)Å attributed to C(22) and is considered to be planar. The dihedral angle between the guest molecule and the host phenyl ring is 64.5(1)°. From the stereoscopic molecular packing diagram (Figure 6.6) it can be seen that there is no evidence of guest parallel stacking either with themselves or with the host phenyl rings.

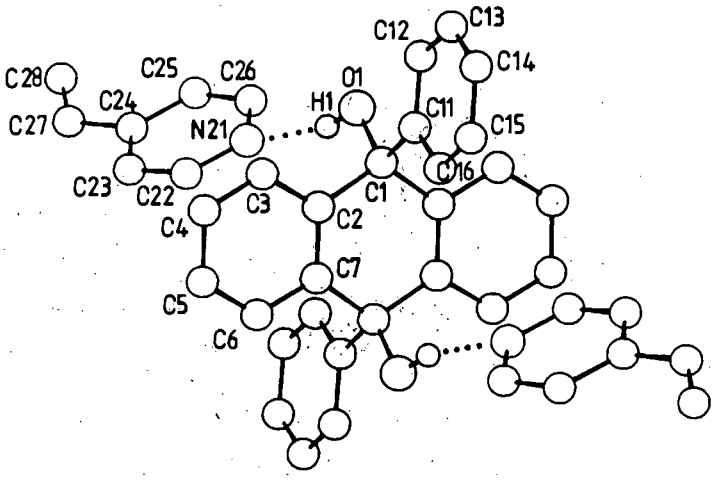

Figure 6.3 Perspective view of Compound (II). For clarity only the hydroxy hydrogen is shown. Dotted lines indicate hydrogen bonds.

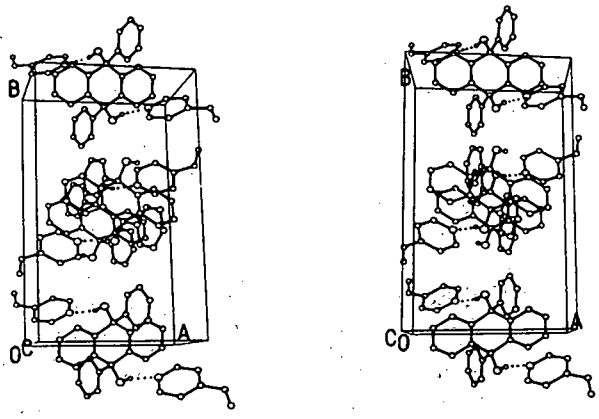

Figure 6.4 Stereoview of molecular packing in Compound (II). For clarity only the hydroxy hydrogen is shown. Hydrogen bonds are indicated by dotted lines.

6.2.4. Compound (IV), $C_{26}H_{20}O_2 \cdot C_6H_7N$

On replacing the guest 4-methylpyridine in (III) by its 2-methylpyridine isomer in (IV), the change in host:guest ratio from 2:1 to 1:1 without a change in space group was unexpected. The larger unit cell volume required the number of formula units, Z, to be 2 with both host molecules situated at centres of symmetry and the guest in a general position.

As stated in section 5.3.5. the guest is disordered and for simplicity the diagrams of the atomic numbering (Figure 6.7) and the stereoscopic molecular packing diagram (Figure 6.8) of (IV) show an average of the two guest positions. This average of the two guest-ring positions yielding a ring orientation intermediate between the two actual disordered positions is depicted in Figure 6.9 . This simplification was achieved by averaging pairs of atomic coordinates excluding those of the methyl substituents.

The two guest-rings are coplanar and related by an approximate mirror plane perpendicular to their mean plane with an N(21)$\cdots$N(31) separation of only 0.54(1)Å. The fact that the two guest-ring orientations are possible implies that the host framework provides a cavity which could accommodate molecules somewhat larger than 2-methylpyridine.

The N(21)- and N(31)- containing rings have maximum out-of-plane deviations of 0.01(1) and 0.02(1)Å respectively and are considered planar taking into account the disordered nature of the 2-methylpyridine.

The dihedral angles between the phenyl ring of the host molecule centred around 0,½,0 and the N(21)- and N(31)- containing guest-ring alternatives are 82.5(3)° and 85.4(3)° respectively. The dihedral angles between the phenyl ring of the other host molecule, centred around 0,½,½, and the N(21)- and N(31)- guest-rings are 64.8(2)° and 65.3(3)° respectively.

Of the four compounds studied in this thesis, compound (IV) is unique in that in addition to host-guest (O-H$\cdots$N) hydrogen bonds, it also contains host-host (O-H$\cdots$O) hydrogen-bonding. These hydrogen bonds shown in Figures 6.7 and

6.8 are represented by dotted lines. The hydrogen bond length and bond angle values are listed in Table 6.1 . The bond lengths and bond angles in Table 6.1 are within acceptable limits.

The host-host hydrogen bonding gives rise to infinite chains of host molecules directly linked along the *z*-direction with every alternate host molecule being hydrogen bonded to two guest molecules (Figure 6.8). As can be seen in the Figure, the infinite *z*-directional host chains are independent of each other.

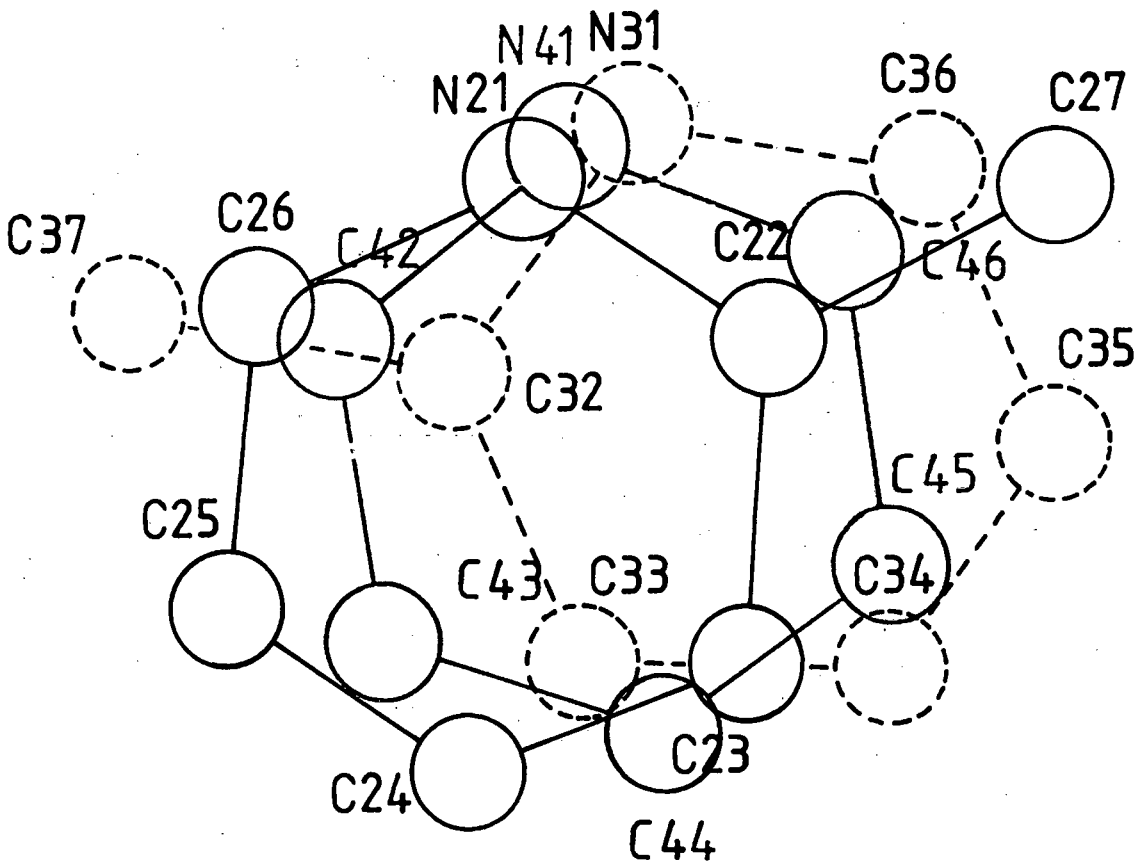

Figure 6.9 Two alternative orientations found for the guest 2-methylpyridine in Compound (IV).

The average position of the two alternative guest orientations. This average position is used in Figures 6.7 and 6.8.

CHAPTER SEVEN

THERMAL ANALYSES

7. THERMAL ANALYSES

7.1. Introduction

Thermogravimetric analysis (TGA) and Differential Scanning calorimetry (DSC) [59,79,80] are complementary techniques in that the information obtained from the one approach is enhanced by the results interpreted from the other method. The results from previous sections, namely single crystal X-ray structure solution and X-ray powder diffraction, on stoichiometry can be confirmed in this section of work. By reconciling thermodynamics with structures, thermal analyses can be used to obtain quantitative information on the interaction energy between host and guest molecules hence establishing a trend for similar compounds. This issue has been discussed for a number of clathrate systems such as Werner clathrates [81] which entrap a variety of organic guest molecules, and the Hofmann clathrates [82] which have been used for chromatographic separation of guest mixtures.

The TGA method employed in this project involves heating a sample at a predetermined linear rate and plotting the weight change as a function of temperature. In host-guest complexes the guest weight % in the sample can be determined from the weight loss prior to host decomposition, taking into account that for this determination to be valid, guest release must occur before host decomposition.

There are a number of factors or conditions that affect the TGA curves with heating rate, atmosphere, sample particle size, nature of the reaction, treatment of the sample and thermal conductivity of the sample included in these to name but a few. If the running conditions for the experiments on all four compounds are the same, this should allow for a good relative comparison of their results. The samples were run under a constant flow of N_2 with a heating rate of 10°C per minute.

The DSC method employed here involves heating a sample at a predetermined rate and comparing the temperature of the sample with that of the reference as a function of increasing furnace temperature. As a reaction occurs, so the heat of reaction results in a difference in temperature between the sample and the reference. This difference is then compensated for by supplying heat to the

sample, in the case of a sample endothermic reaction (plotted as a negative peak), or to the reference, in the case of a sample exotherm (plotted as a positive peak). The Du Pont instrument used then calculates the heat flow (W/g) for the reaction and plots heat flow versus furnace temperature. The enthalpy of a reaction is proportional to the area under the peak.

Upon guest release from a host-guest complex or host melting, the entropy of the system increases, combined with a positive enthalpy change which can be seen in the following section on DSC results. The opposite i.e. guest inclusion into a host lattice, would result in a decrease in entropy combined with a negative enthalpy change being observed.

As is the case with TGA there are a number of factors that can affect the DSC curves including heating rate, atmosphere, the sample holder, thermocouple location, particle size and sample packing.

The machine running conditions and sample preparations were kept constant and with the sample and particle size of the same order for all four compounds, comparison of their results to establish trends is valid.

7.2. TGA and DSC results

The TGA and DSC plots of compounds (I) to (IV) are shown in Figures 7.1 to 7.4 and a summary of the results drawn from these Figures listed in Tables 7.1 for the TGA and 7.2 and 7.3 for the DSC results.

Compound (I) having a 1:1 host:guest ratio has a theoretical guest weight % of 16.5 . From Figure 7.1 it can be seen that from 69 to 110°C, 16.5% weight loss is observed. At about 250°C the weight % starts to decrease again and this is attributed to host decomposition.

From Figure 7.1 we can see that the DSC results of compound (I) and the TGA results are complementary. The DSC shows a relatively broad negative peak starting at 69°C with a minimum at 98°C. The area under the endothermic peak gives the enthalpy change upon guest loss (Table 7.2) from the host-guest compound. The sharp endothermic peak starting at 263°C corresponds to the

Table 7.1 TGA results for Compounds (I) to (IV)

	Reaction	Onset Temp./ °C	Calculated Weight Loss/ %	Measured Weight Loss/ %
	Compound (I)			
1.	$H \cdot C_4H_8O \rightarrow H + C_4H_8O$	69	16.5	16.5
	Compound (II)			
2.	$H \cdot 2C_7H_7N \rightarrow H + 2C_7H_7N$	110	36.6	36.1
	Compound (III)			
3.	$H \cdot 2C_6H_7N \rightarrow H \cdot C_6H_7N + C_6H_7N$	82	16.8	16.2
	$H \cdot C_6H_7N \rightarrow H + C_6H_7N$	135	33.6	32.5
	Compound (IV)			
4.	$H \cdot C_6H_7N \rightarrow H + C_6H_7N$	137	20.4	21.5

$H = C_{26}H_{20}O_2$

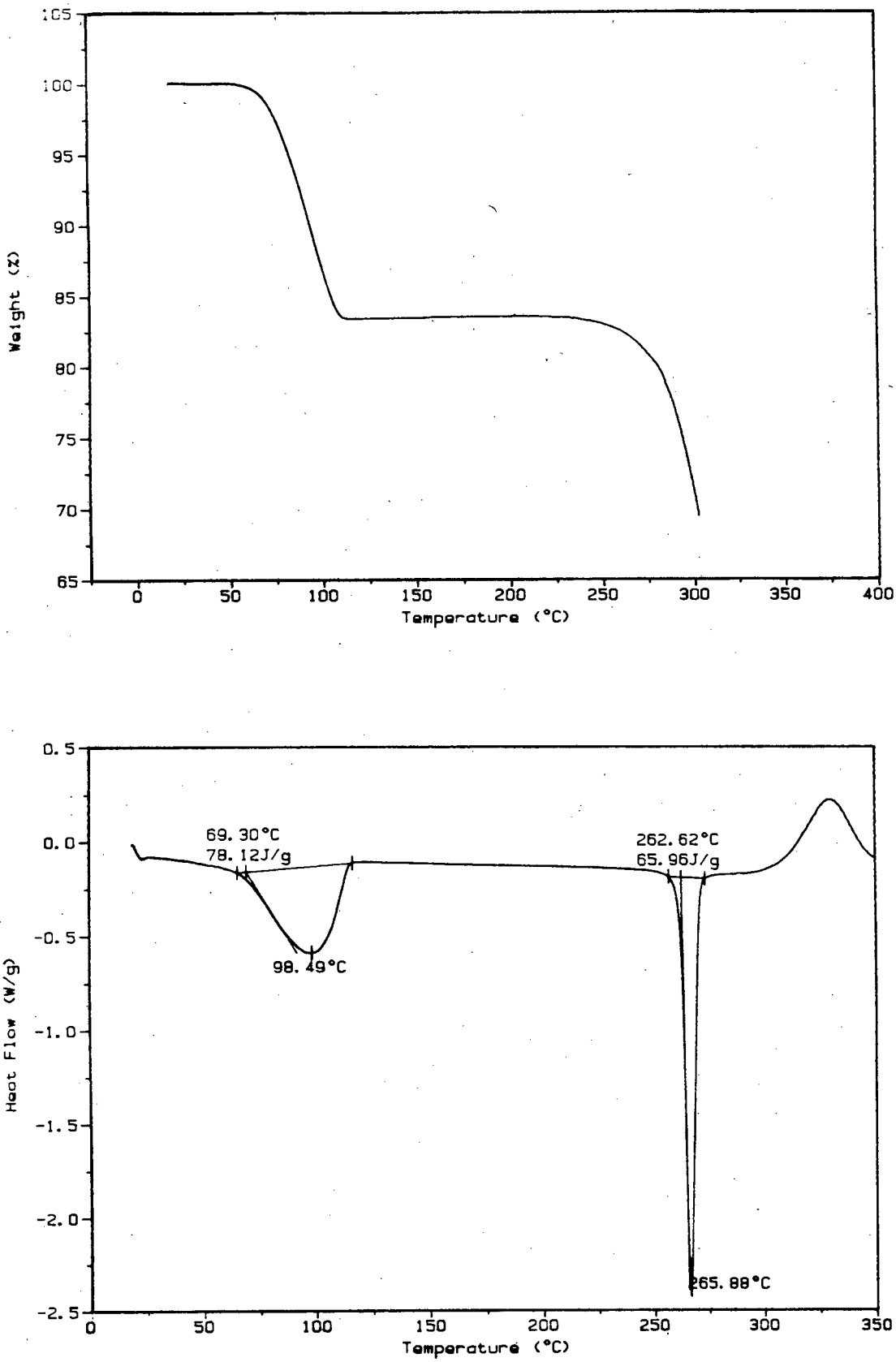

Figure 7.1 TGA and DSC Curves of Compound (I)

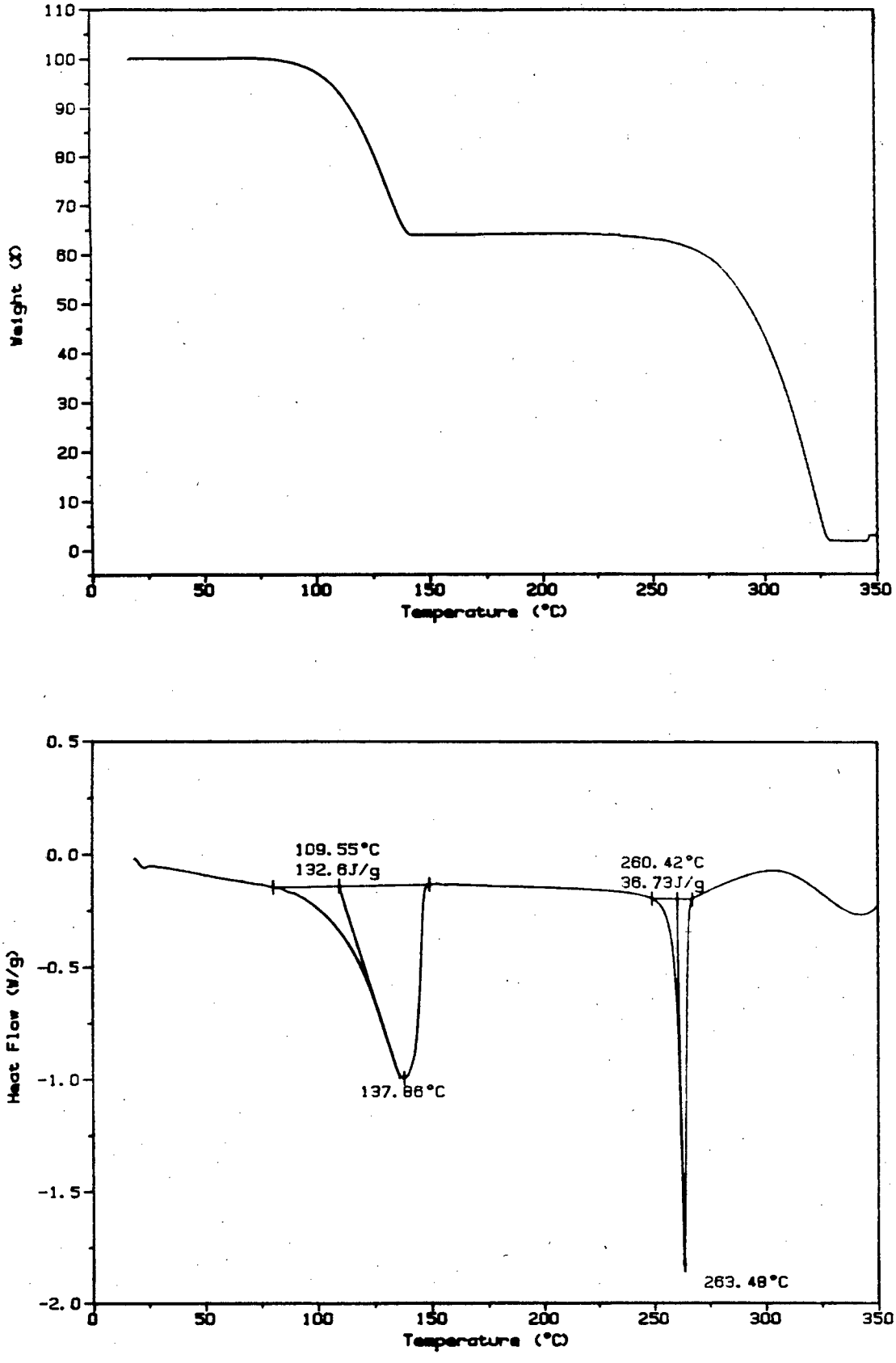

Figure 7.2 TGA and DSC Curves of Compound (II)

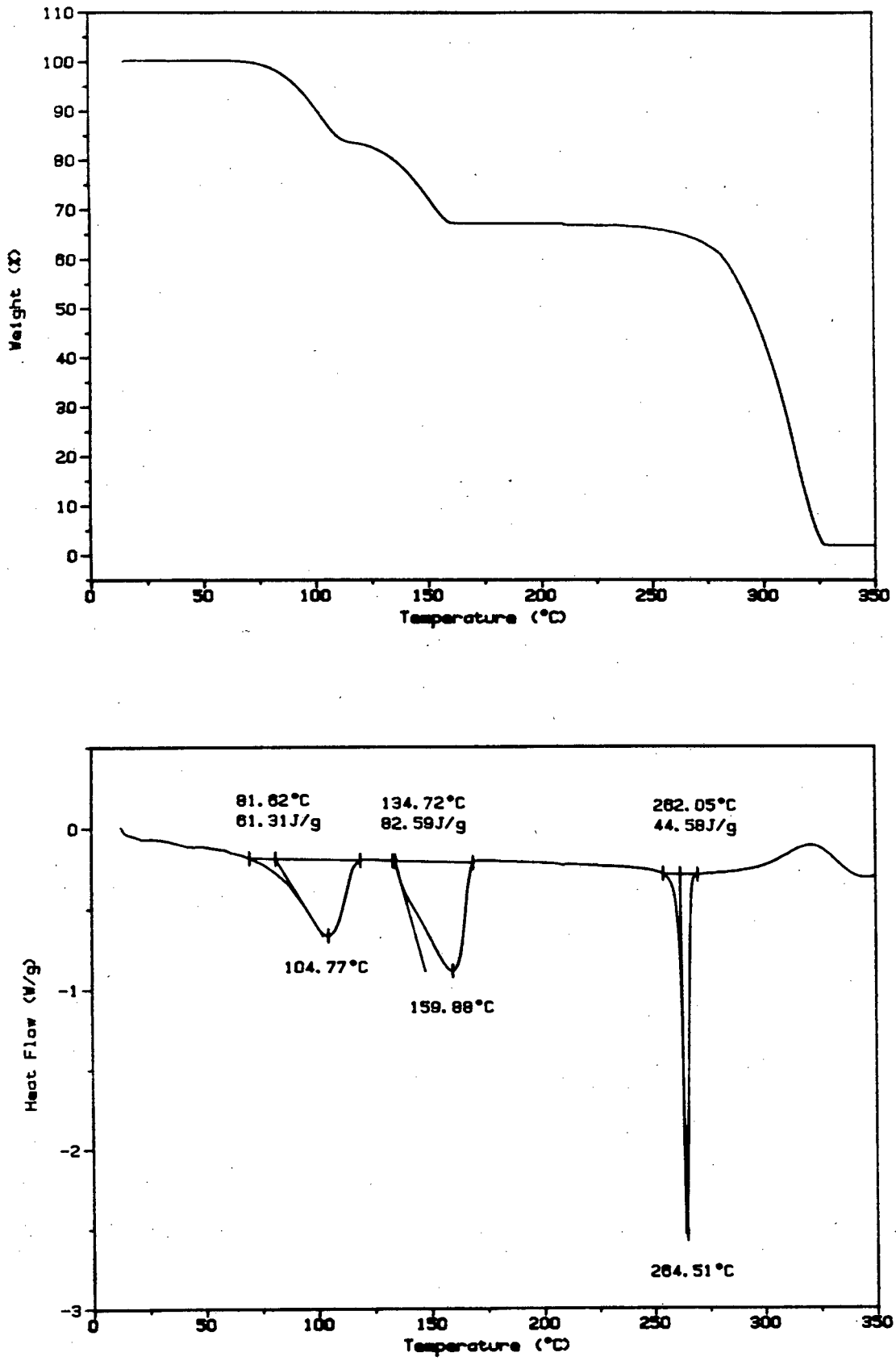

Figure 7.3 TGA and DSC Curves of Compound (III)

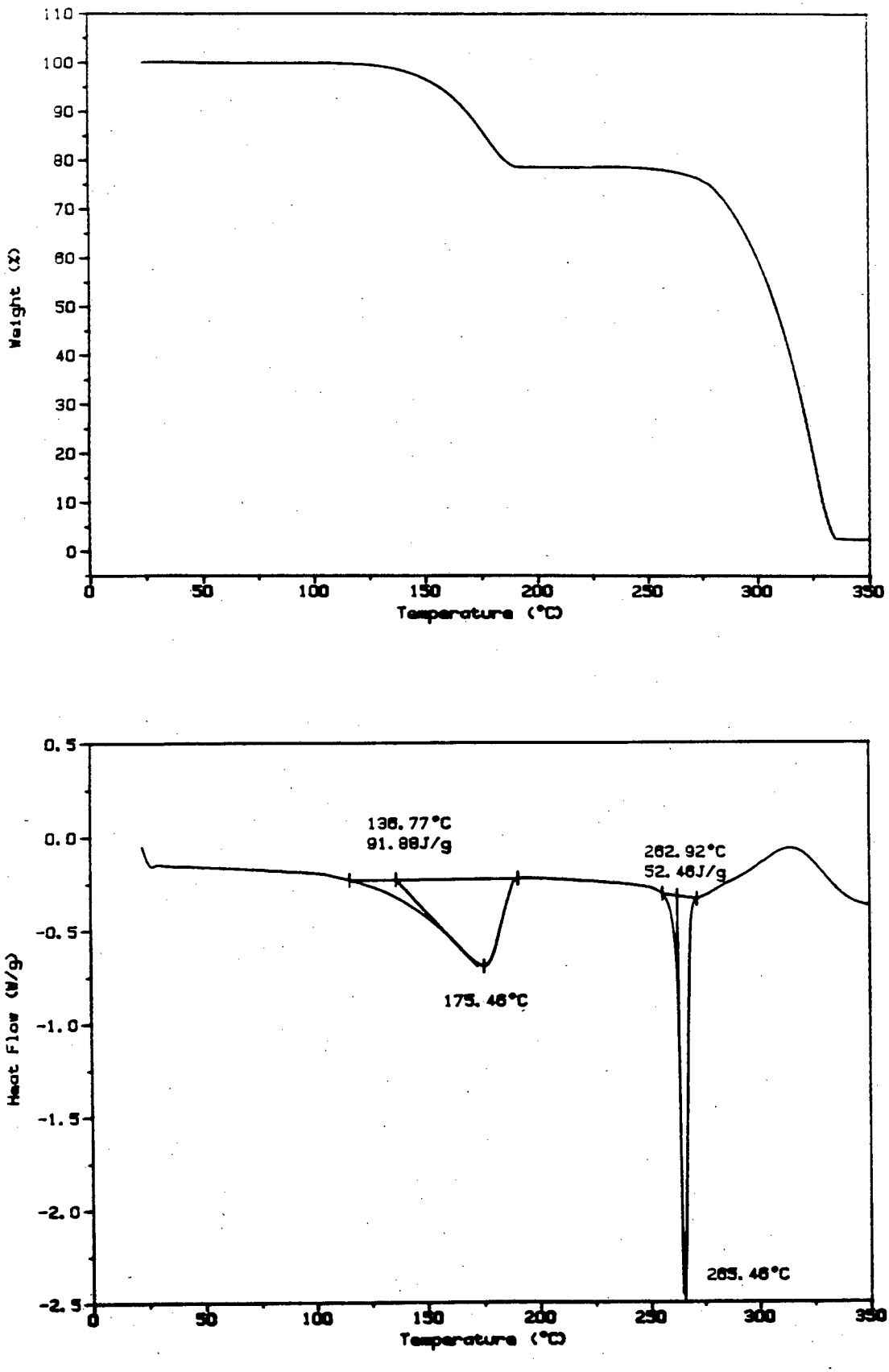

Figure 7.4 TGA and DSC Curves of Compound (IV)

melting point of the guest-free host confirmed by the melting point of the synthesised host in section 3.1. .

Compounds (II) and (IV) give very similar results to those exhibited by compound (I). Compound (II) (Figure 7.2) has a 2:1 host:guest ratio but loses both guest molecules in a single step starting at 110°C. The calculated and measured weight loss differ by only 0.5% . Compound (IV) (Figure 7.7) loses its guest in one step commencing at 137°C. The difference in calculated and measured weight loss is 1.1% . Both (II) and (IV) have sharp endothermic peaks at around 260-263°C, again corresponding to the melting and subsequent decomposition of the guest-free host.

Compound (III) has a host:guest ratio of 1:2. From the structure solution of (III) it can be seen that these two guest molecules are equivalent, being related by a centre of symmetry. From the TGA and DSC results (Figure 7.5) it is evident that the guest molecules are released in a two-stage process. The weight % of the guest in (III) is 33.6% thereby giving each guest molecule a weight % of 16.8 . The weight % lost in the first step of the TGA is 16.2% (onset temperature of 82°C) and in the second step the loss is 16.3% . The conclusion drawn from these results is that one guest molecule is lost whereupon the host and the remaining guest molecule rearrange to form a new host-guest lattice (see chapter 4). The remaining guest molecule is then released (starting at 135°C) from the new host-guest lattice leaving the guest-free host to finally melt and decompose at 262°C.

The reason that the enthalpy values (Table 7.2) for the two steps are different, even though the TGA shows that the same amount of guest is being lost, is as a result of the guest being released from two different host lattices requiring differing amounts of energy.

On doing melting point determinations on the hotstage, the guest loss for all four compounds could not be seen as a dramatic effect but rather as a slow change in the crystal from clear to opaque around the temperature range of guest loss, followed by a melting at around 262°C.

Table 7.2 DSC results for Compounds (I) to (IV)

Reaction	Onset Temp./ °C	ΔH/ Jg^{-1}	ΔH/ $kJmol^{-1}$	O-H····O/ O-H····N/ Å
Compound (I)				
1. $H \cdot C_4H_8O \rightarrow H + C_4H_8O$	69	78.1	34.1	2.721(6)
Compound (II)				
2. $H \cdot 2C_7H_7N \rightarrow H + 2C_7H_7N$	110	132.6*	72.2*	2.841(4)
Compound (III)				
3. $H \cdot 2C_6H_7N \rightarrow H \cdot C_6H_7N + C_6H_7N$	82	61.3	33.8	2.817(3)
$H \cdot C_6H_7N \rightarrow H + C_6H_7N$	135	82.6	45.5	
Compound (IV)				
4. $H \cdot C_6H_7N \rightarrow H + C_6H_7N$	137	91.9	42.1	2.831(6) 2.656(6)

$H = C_{26}H_{20}O_2$

* = value for the release of two guest molecules.

Table 7.3 Normalised DSC results for Compounds (II) to (IV)

	Reaction	ΔH/ kJmol^{-1} (Melting Pt.)	ΔH/ kJmol^{-1} (Guest release)	ΔH/ kJmol^{-1} (Normalised G release)	O-H···O/ O-H···N/ Å
	Compound (II)				
2.	$H \cdot 2C_7H_7N \rightarrow H + 2C_7H_7N$	21.1	76.2*	76.2*	2.841(4)
	Compound (III)				
3.	$H \cdot 2C_6H_7N \rightarrow H \cdot C_6H_7N + C_6H_7N$	24.6	33.8	29.0	2.817(3)
	$H \cdot C_6H_7N \rightarrow H + C_6H_7N$	24.6	45.5	39.0	
	Compound (IV)				
4.	$H \cdot C_6H_7N \rightarrow H + C_6H_7N$	24.0	42.0	36.9	2.831(6) 2.656(6)

H = $C_{26}H_{20}O_2$

G = guest

* = value for the release of two guest molecules.

From the DSC study one might expect correlation between the O····N hydrogen bond distance and the ΔH value of the guest release reaction for compounds (II), (III) and (IV) (Table 7.2). However there are difficulties in determining a trend for these three compounds. Compound (II) releases both guests in a single step with a ΔH value of 72.2 kJmole^{-1} or 36.1 kJ per guest molecule. Compound (III) as mentioned earlier releases the two guests in two stages having ΔH values 33.8 and 45.5 kJmol^{-1} respectively, averaging to 39.7 kJmol^{-1}. With compound (IV), the guest molecule is disordered with the two alternative O····N distances averaging to 2.744(6)Å, associated with a ΔH value of 42.1 kJmol^{-1}. Using these values, it could be argued that there is a qualitative inverse correlation between O····N hydrogen bond length and the ΔH value of the guest release reaction.

An alternative argument is that the ΔH values of guest release should be normalised based on their melting point enthalpies. This is assuming that the state of the host after guest release is the same for all three compounds. This was established in Chapter 4 as they all collapse back to the α-phase on guest release. The normalised values in Table 7.3 show that there is in fact no correlation between O····N hydrogen bond length and ΔH of guest release. In Table 7.3 the enthalpy value representing guest release from compound (III) corresponds to the first step of the two-stage guest release process. Although compound (III) has a two-step guest loss process, only the first should be considered as the second guest is released from a host lattice structure (the γ-phase, see Chapter 4) which is unknown, as is the O····N hydrogen bond length.

Further work would have to be carried out on a variety of substituted pyridines to confirm the existence of any trend.

CHAPTER EIGHT

CONCLUSION

8. CONCLUSION

Based on the information gained from the X-ray crystal structures of the four compounds, the classification of these compounds in terms of the system proposed by Weber and Josel [15,16] as discussed in the introduction is not very definitive. These host-guest aggregates are derived from a coordination between host and guest and are thus classed as complexes. Further classification in terms of their topology is difficult as no definite channel or cavity shapes were obvious. In Chapter 6 it was stated that for compound (I) it appears as if the guest molecules, 2-butanone, occupy channels parallel to [001]. Energy calculations of the movement of the guest through this supposed channel using the program EENY [83] were carried out. In these calculations the guest was allowed to tumble (i.e. change its orientation in accord with a minimum energy criterion) as it progressed through the cell. The host phenyl groups were also allowed to rotate around the bonds linking them to the central tricyclic system. These calculations showed that small translations of the guest to either side of the energy minimum (i.e. the position determined crystallographically) were unconstrained, but on translating the guest from one unit cell to the next along [001] the resulting close approach of the host and guest molecules led to very high energy barriers being encountered. This indicated that the guest molecules do not reside in channels, but rather in confined regions constricted along the [001] direction by host molecules. The absence of a channel was confirmed by inspection of a space-filling diagram of the host molecules viewed along [001].

The host:guest ratios of 1:1, 1:2, 1:2, and 1:1 for compounds (I), (II), (III), and (IV) respectively were confirmed from the X-ray powder diffraction studies, crystal structure solutions, density measurements, microanalyses and thermal analyses.

The host lattice structure on going from guest inclusion to guest release and finally host melting and subsequent decomposition was investigated. From the guest desorption studies, structure solutions and the thermal analyses, the following conclusions are drawn. On heating compounds (I), (II) and (IV) the guest is released in a single step accompanied by host rearrangement to the original α-phase, exhibited by the host in a guest-free environment. Compounds (I) and (II) have host-guest hydrogen-bonding but no specific hydrogen-bonding interaction between the host molecules. When the guest is released from the host-guest compound these hydrogen bonds are broken leaving no structural

support to keep the β-phase framework intact. This, together with the fact that if the guest does not reside in a relatively large channel, it has to break its way out, results in the β-phase collapsing back to the α-phase. In addition to host-guest hydrogen-bonding, compound (IV) also has host-host hydrogen-bonding giving rise to infinite chains of host molecules which could support the host lattice on guest departure resulting in the "empty" β_o-phase being observed. Although the disordered nature of the 2-picoline guest indicates that the lattice void could accommodate a larger guest molecule, the escape of the guest molecule must be hindered and the host lattice structure is broken as a consequence, leaving compound (IV) to revert back to the α-phase.

The guest loss from (III) is a two-step process. Upon heating, the equivalent of one guest molecule per unit cell is released. This is accompanied by a host rearrangement to some other structure, known as the γ-phase, incorporating the second, as yet unreleased, guest molecule. Further heating is required to release the guest from this new host structure which then reverts back to the α-phase on the loss of the remaining guest.

The "empty" β_o-phase was not exhibited by any of the four compounds studied, hence their inability to act as separating agents when loaded onto a G.C. column (as discussed in the introduction).

Further studies would include attempts to isolate and solve the crystal structure of the previously mentioned γ-phase host-(4-picoline) guest in the 1:1 ratio exhibited after one guest molecule is released from (III). This could be attempted by growing crystals of trans-9,10-dihydroxy-9,10-diphenyl-9,10-dihydroanthracene and 4-picoline in a 1:1 ratio in various organic solvents and solving the crystal structure by X-ray methods.

The crystal structure of the host-(3-picoline) complex in a 1:2 host:guest ratio has recently been solved by co-workers [84]. This crystal structure is not isomorphous with that of the host-(4-picoline) crystal structure and hence their lattice energies would differ. In competition experiments, this lattice energy difference could lead to preferential inclusion of one of the isomers into the host lattice. Such a competition experiment would involve a study of the crystals grown from a solution of the host in a mixture of the two isomers. Should preferential uptake of one of the isomers be exhibited, this technique could be used to separate the 3- and

4-picoline isomers (b.p. of 143.5 and 143.1°C respectively).

A thermal study of the host with a variety of substituted pyridines e.g. 3-picoline, lutidines, other vinylpyridines and even nitriles should be carried out to help establish a trend between O····N hydrogen bond length and the enthalpy value associated with guest release.

REFERENCES

REFERENCES

1. Powell, H.M. (1948) *J. Chem. Soc.*, p61.

2. Davy, H (1811) *Philos. Trans. R. Soc. London*, **101**, p1.

3. Faraday, M. (1823) *Quart. J. Sci.*, **15**, p71.

4. Schafhäutl, C. (1841) *J. Prakt. Chem.*, **21**, p129.

5. Wohler, F. (1849) *Ann. Chem. Liebigs*, **69**, p297.

6. Villiers, A. (1891) *C.R. Hebd. Sceances Acad. Sci.*, **112**, p536.

7. Hofmann, K.A. and Küspert, F. (1897) *Z. Anorg. Allg. Chem.*, **15**, p204.

8. Hartley, H. and Thomas, N.G. (1906) *J. Chem. Soc.*, p1013.

9. Spallino, R. and Provenzal, G. (1909) *Gazz. Chim. Ital.*, **39**, p325.

10. Dianin, A.P. (1914) *J. Soc. Phys. Chem. Russe*, **46**, p1310.

11. Wieland, H. and Sorge, H. (1916) *Z. Physiol. Chem. Hoppe-Seyler's*, **97**, p1.

12. Terres, E. and Vollmer, W. (1935) *Z. Petroleum*, **31**, p1.

13. Bengen, M.F. (1940) German Patent Application, OZ 123438.

14. Mikus, F.F., Hixon, R.M. and Rundle, R.E. (1946) *J. Am. Chem. Soc.*, **63**, p1115.

15. Weber, E. and Josel, H.-P. (1983) *J.Incl. Phenom.* **1**, p79.

16. Weber, E. (1987) Topics in Current Chemistry, **140**, p2.

17. Goldberg, I. (1984) Inclusion Compounds, Vol 2, Atwood, Davies and MacNicol, eds., Academic Press, London, Chap. 9, p261.

18. Metz, B., Moras, D. and Weiss, R. (1970) *J. Chem. Soc., Chem. Commun.*, p217.

19. MacNicol, D.D. (1984) Inclusion Compounds, Vol 2, Atwood, Davies and MacNicol, eds., Academic Press, London, Chap. 1, p1.

20. Takemoto, K. and Sonoda, N. (1984) Inclusion Compounds, Vol 2, Atwood, Davies and MacNicol, eds., Academic Press, London, Chap. 2, p47.

21. Lalancette, J.-M., Rollin, G. and Daumas,P. (1972) *Can. J. Chem.*, **50**, p3058.

22. Davies, J.E.D. (1981) *J. Molecular Structure*, **75**, p1.

23. Thomas, J.M., Adams, J.M., Graham, S.H. and Tennakoon, D.T. (1977) Solid State Chemistry of Energy Conversion and Storage, Advances in Chemistry Series 163, American Chem. Soc., Goodenough, J.B. and Whittingham, M.S., eds., p298.

24. Whittingham, M.S. and Chianelli, R.R. (1980) *J. Chem. Educ.*, **57**, p569.

25. Iwamoto, T., Nakano, T., Morita, M., Miyoshi, T., Miyamoto, T. and Sasaki, Y. (1968) *Inorg. Chim. Acta.*, **2**, p313.

26. Schaeffer, W.D., Dorsey, W.S., Skinner, D.A. and Christian, C.G. (1957) *J. Am. Chem. Soc.*, **79**, p5870.

27. Lipkowski, J., Pawlowska, M. and Sybilska, D. (1979) *J. Chromatog.*, **176**, p43.

28. Smolkavà-Keulemansovà, E. and Krysl, S. (1980) *J. Chromatog.*, **184**, p347.

29. Davies, J.E.D. (1977) *J. Chem. Educ.*, **54**, p536.

30. Arad-Yellin, R., Green, B.S., Knossow, M. and Tsoucaris, G. (1984) Inclusion Compounds, Vol 3, Atwood, Davies and MacNicol, eds., Academic Press, London, Chap. 9, p264.

31. Davies, J.E.D., Kemula, W.,Powell, H.M. and Smith, N.O. (1983) *J. Incl. Phenom.*, **1**, p3.

32. Saenger, W. (1980) *Angew. Chem., Int. Ed. Engl.*, **19**, p344.

33. Szejtli, J. (1984) Inclusion Compounds, Vol 3, Atwood, Davies and MacNicol, eds., Academic Press, London, Chap. 11, p331.

34. Hiroshi, T. and Miwa, I. (1977) K. Japan. Kokai, 76 108641, (*Chem. Abs.* **86**, 31101).

35. Schlenk, H., Sonol, D.M. and Tillotson, J.A. (1958) U.S.P. 2 827 452, (*Chem. Abs.* **52**, 12901).

36. MacNicol, D.D., McKendrick, J.J. and Wilson, D.R. (1978) *Chem. Soc. Rev.*, **1**, p65.

37. Dewar, M.J.S., Nahlovsky, B.D. (1974) *J. Am. Chem. Soc.*, **96**, p460.

38. Arad-Yellin, R., Brunie, S., Green, B.S., Knossov, M. and Tsoucaris, G. (1979) *J. Am. Chem. Soc.*, **101**, p7529.

39. Parsonage, N.G. and Staveley, L.A.K. (1984) Inclusion Compounds, Vol 3, Atwood, Davies and MacNicol, eds., Academic Press, London, Chap. 1, p1.

40. Saenger, W. (1974) *Umschau*, **74**, p635.

41. Frömming, K.H. (1973) *Pharm. uns. Zeit.*, **2**, p109.

42. MacNicol, D.D. and Wilson, D.R. (1976) *J. Chem. Soc. Chem. Commun.*, p494.

43. MacNicol, D.D. (1984) Inclusion Compounds, Vol 2, Atwood, Davies and MacNicol, eds., Academic Press, London, Chap. 5, p123.

44. Toda, F. and Akagi, K. (1968) *Tetrahedron Lett.*, p3695.

45. Toda, F., Tanaka, K. and Mak, T.C.W. (1985) *J. Incl. Phenom.*, **3**, p225.

46. Toda, F. Tanaka, K. and Mak, T.C.W. (1985) *Bull. Chem. Soc. Japan*, Vol. 58, No.8, p2221.

47. Toda, F., Ward, D.L. and Hart, H. (1981) *Tetrahedron Lett.*, **22**, p3865.

48. Toda, F. Tanaka, K. and Mak, T.C.W. (1984) *Tetrahedron Lett.*, **25**, p1359.

49. Toda, F. (1987) Topics in Current Chemistry, **140**, p43.

50. Toda, F., Tanaka, K., Ulibarri Daumas, G. and Sanchez, M.C. (1983) *Chem. Lett.*, **10**, p1521.

51. Shin, J.M., Toda, F. and Jhon, M.S. (1987) *J. Incl. Phenom.*, **5**, p567.

52. Barrer, R.M. (1978) Zeolites and Clay Minerals as Sorbents and Molecular Sieves, Academic Press, London.

53. Taylor, M.W. (1988) PhD. Thesis, Univ. of Cape Town.

54. Toda, F., Tanaka, K., Nagamatsu, S. and Mak, T.C.W. (1985) *Isr. J. Chem.*, **25**, p346.

55. Bond, D.R., Nassimbeni, L.R. and Toda, F. (1989) *J. Incl. Phenom. and Molec. Recognition in Chem.*, **7**, p623.

56. Bond, D.R., Nassimbeni, L.R. and Toda, F. (1989) *J. Crystallogr. and Spectroscopic Research*, Vol 19, No.5, p847.

57. Ingold, C.K. and Marshall, P.G. (1926) *J. Chem. Soc.*, **II**, p3080.

58. Monar, I. (1972) *Mikrochimica Acta.*, **6**, p784.

59. Wendlandt, W.W.M. (1986) Chemical Analysis, Vol 19, Elving, P.J., Winefordner, J.D. and Kolthoff, I.M. eds., Wiley-Interscience Publishers, New York.

60. Wendlandt, W.W.M. (1962) *Anal. Chim. Acta.*, **27**, p309.

61. "Operators Manual" (1985) Du Pont Instruments, Differential Scanning Calorimeter 910, Du Pont Co., Instrument Systems, Wilmington.

62. Weast, R.C., Astle, M.J. and Beyer, W.H. eds. (1985) CRC Handbook of Chemistry and Physics, CRC Press, Inc., Florida.

63. McBain, J.W. and Bakr, A.M. (1926) *J. Am. Chem. Soc.*, **48**, p690.

64. Sheldrick, G.M. (1976) SHELX-76. Program for crystal structure determination, University of Cambridge, Cambridge, England.

65. Sheldrick, G.M. (1986) SHELX-86. Program for the solution of crystal structures from diffraction data. Univ. of Göttingen, Federal Republic of Germany.

66. Klyne, W. and Prelog, V. (1960) *Experientia*, **16**, p521.

67. Nardelli, M., Musatti, A., Domiano, P. and Andreetti, G. (1965) Ric. Sci., 15(II-A), p807.

68. Nardelli, M. (1983) *Comput. Chem.*, **7**, p95.

69. Gabe, E.J., Lee, F.L. and Le Page, Y. (1985) Crystallographic Computing 3, Sheldrick, G.M., Krüger, C. and Goddard, R. eds., Clarendon Press, Oxford, p167.

70. "Harvard Graphics", Software Publishing Corporation, Mountain View, CA 94043, U.S.A.

71. Cromer, D.T. and Mann, J.B. (1968) *Acta Crystallogr.*, **A24**, p321.

72. Stewart, R.F., Davidson, E.R. and Simpson, W.T. (1965) *J. Chem. Phys.*, **42**, p3175.

73. Cromer, D.T. and Liberman, D. (1970) *J. Chem. Phys.*, **53**, p1891.

74. De Titta, G.T., Edmonds, J.W., Langs, D.A. and Hauptman, H. (1975) *Acta Crystallogr.*, **A31**, p472.

75. Herbstein, F.H., Kapon, M. and Reisner, G.M. (1986) *Acta Crystallogr.*, **B42**, p181.

76. Duax, W.L. and Norton, D.A.,eds. (1975) Atlas of Steroid Structure, Vol 1, Plenum Press, London.

Brammer, L., Orpen, G.A. and Taylor, R.

77. Allen, F.H., Kennard, O. ~~and~~ Watson, D.G., (1987) *J.Chem. Soc. Perkin Trans II*, pS1.

78. Bondi, A. (1964) *J. Phys. Chem.*, **64**, p441.

79. Brown, M.E. (1988) Introduction to Thermal Analysis, Techniques and Applications, Chapman and Hall, New York.

80. Byrn, S.R. (1982) Solid State Chemistry of Drugs, Academic Press, New York.

81. Moore, M.H., Nassimbeni, L.R. and Niven, M.L. (1987) *Inorg. Chim. Acta.*, **131**, p45.

82. Sopkovà, A. and Šinglair, M (1984) Inclusion Compounds, Vol 3, Atwood, Davies and MacNicol, eds., Academic Press, London, Chap. 7, p245.

83. Motherwell, W.D.S. (1974) EENY - Potential Energy Program, Cambridge, unpublished.

84. Schubert, W. and Nassimbeni, L.R. (1990) unpublished results.

85. Germain, G., Main, P. and Woolfson, M.M. (1970) *Acta Crystallogr.* **B26**, p274.

APPENDICES

APPENDIX 1. Mathematical expressions

Density equation (section 3.3.1. and 5.1)

$$Z_H M_H + Z_G M_G = D_m V N_A$$

Z_H = number of host molecules per unit cell.
M_H = molecular weight of the host molecule (g/mol).
Z_G = number of guest molecules per unit cell.
M_G = molecular weight of the guest molecule (g/mol).
D_m = measured density (g/cm^3)
V = unit cell volume (cm^3)
N_A = Avogadro's number , 6.02204×10^{23} (/mol)

Equations for calculations of asymmetry parameters for mirror related, and two -fold axis related torsion angles, ΔC_S and ΔC_2 respectively (section 6.1.) [76]

$$\Delta C_S = \{ \sum_{i=1}^{m} (\psi_i + \psi_i')^2 / m \}^{1/2}$$

$$\Delta C_2 = \{ \sum_{i=1}^{m} (\psi_i - \psi_i')^2 / m \}^{1/2}$$

m = number of individual ψ_i, and ψ_i' comparisons
ψ_i, ψ_i' = torsion angles related by mirror plane or two-fold axis

Significance test (chapter 6)

If, for two parameters, $q_1 \pm \sigma(q_1)$ and $q_2 \pm \sigma(q_2)$, the difference

$$|q_1 - q_2| > 3 \{\sigma^2(q_1) + \sigma^2(q_2)\}^{1/2}$$

then q_1 and q_2 are judged to be significantly different.

APPENDIX 2. R value expressions

$R_{(int)} = \{[\Sigma(N\Sigma(w(F_{mean} - F)^2))]/[\Sigma((N - 1)\Sigma(wF^2))]\}^{½}$

where the inner summations are over the N equivalent reflections averaged to give F_{mean}, and the outer summations are over all unique reflections.

$R_A = (\Sigma A\alpha)^2/[(\Sigma A^2)(\Sigma\alpha^2)]$ [85]

where α is the strength of an indication defined by:

$$\alpha = \{[\Sigma_{kr}\kappa(h,k)\cos(\phi_k + \phi_{h-k})]^2 + [\Sigma_{kr}\kappa(h,k)\sin(\phi_k + \phi_{h-k})]^2\}^{½}$$

and A is the estimated value of α.

$R = (\Sigma||F_o| - |F_c||)/(\Sigma|F_o|)$

$R_w = (\Sigma w^{½}||F_o| - |F_c||)/(\Sigma w^{½}|F_o|)$

MICROFICHE

APPENDIX 3

Table 3.1.1. Compound (I) - Bond lengths
Table 3.1.2. Compound (I) - Bond angles
Table 3.1.3. Compound (I) - Torsion angles
Table 3.2.1. Compound (II) - Bond lengths
Table 3.2.2. Compound (II) - Bond angles
Table 3.2.3. Compound (II) - Torsion angles
Table 3.3.1. Compound (III) - Bond lengths
Table 3.3.2. Compound (III) - Bond angles
Table 3.3.3. Compound (III) - Torsion angles
Table 3.4.1. Compound (IV) - Bond lengths
Table 3.4.2. Compound (IV) - Bond angles
Table 3.4.3. Compound (IV) - Torsion angles

APPENDIX 4

Table 4.1. Compound (I) - Least-squares planes
Table 4.2. Compound (II) - Least-squares planes
Table 4.3. Compound (III) - Least-squares planes
Table 4.4. Compound (I) - Least-squares planes

APPENDIX 5

Observed and calculated structure factors

APPENDIX 6

Analysis of variance